CYSTATIN RELATED EPIDIDYMAL SPERMATOGENIC PROTEIN RESIDES IN THE OUTER DENSE FIBRES AND LIKELY TRANSIENTLY ASSOCIATES WITH THE SURFACE OF EPIDIDYMAL MOUSE SPERMATOZOA

by

Marvin Ferrer

A thesis submitted to the Department of Anatomy and Cell Biology

In conformity with the requirements for

the degree of Master of Science

Queen's University

Kingston, Ontario, Canada

August, 2010

Your file Votre référence
ISBN: 978-0-494-70254-3
Our file Notre référence
ISBN: 978-0-494-70254-3

Abstract

Cystatin Related Epididymal Spermatogenic protein (CRES) is expressed in both the testis and epididymis and found associated with spermatozoa. It appears as non-glycosylated (14 and 12 kDa) and glycosylated isoforms (19 and 17 kDa). The role of CRES is enigmatic and dependent on localization of its isoforms, which is the objective of this study. The initial approach was to investigate testicular and epididymal origins of these isoforms by immunohistochemistry and immunogold cytochemistry. To further pinpoint CRES localization we then selectively extracted and fractionated epididymal spermatozoa in order to find by immunoblotting which sperm fractions contained CRES isoforms. Immunohistochemical analysis of mouse spermatogenesis showed that CRES was expressed in the tail cytoplasm of elongating spermatids from step 9-16, with a pattern reminiscent of outer dense fibre (ODF) proteins. Ultrastructural immunocytochemistry revealed that the immunogold label was concentrated over growing ODFs and mitochondrial sheath in the testes which persisted in spermatozoa through the epididymis. Sequential extractions of isolated sperm tails with Triton X-100-dithiothreitol (DTT) to remove the mitochondrial sheath, whose extract contained an unrelated 66 kDa immunoreactive band, followed by either sodium dodecyl sulfate (SDS)-DTT or urea-DTT to solubilise accessory fibres of the tail revealed a 14 kDa immunoreactive band associated with the ODF. In addition, Western blots revealed glycosylated and non-glycosylated CRES isoforms in nonyl phenoxylpolyethoxylethanol (NP40) extracts of the caput, but not cauda, sperm. Immunohistochemical analysis of the caput and cauda epithelium showed that CRES is secreted by the Golgi apparatus of the

initial segment, fills the proximal caput lumen, and disappears by mid caput. Western blots of caput and cauda tissue and luminal fluid revealed 14 and 19 kDa immunoreactive bands in caput tissues and luminal fluid, but not in the cauda. This study concludes that there are two origins of CRES, one arising in the testis and the other in the epididymis. Testicular CRES is ionically and covalently associated with the ODF while epididymal CRES is detergent soluble and is most likely associated temporarily with the surface of caput epididymal sperm.

Acknowledgments

I would like to thank my supervisor, Dr. Richard Oko, for his guidance and help in preparing this project. I am very grateful for the many opportunities which he has provided me. I would also like to thank the past and present members of the Oko lab. Wei Xu taught me Western blots and helped tremendously with data analysis, Yang Yu frequently helped me obtain samples, and Judy Vanhorne's patience and amazing guiding hand allowed me to learn numerous techniques as well. Lastly, Mahmoud Aarabi, Hilma Rodriguez, Bethany Oeming, Zheng Qin, and Gareth Hammond have all made the lab a wonderful place to work with their humour and friendship.

Dr. Gail Cornwall of Texas Tech University has been very generous in providing samples and antibody for my project. She was the one who initiated this project, which has been very challenging and exciting. I really appreciate her guidance and insight and I am tremendously grateful for her help.

I would also like to offer thanks to the staff of the Department of Anatomy and Cell Biology, and to the instructors which I have had the pleasure of learning from over the duration of my studies.

Lastly, I would like to thank my amazing friends and family for their support. Without them, I could never have made it to where I am now, and would never be able to get to where I want to go in the future.

Table of Contents

List of Figures

List of Abbreviations

ABC	avidin-biotin-peroxidase complex
anti-CRES	polyclonal affinity purified rabbit anti-mouse CRES antibody
ATP	adenosine triphosphate
cAMP	cyclic adenosine monophosphate
CASA	computer-aided sperm analysis
CRES	cystatin-related epididymal spermatogenic protein
DAB	diaminobenzidine tetrahydrochloride
DTT	dithiothreitol
EDTA	ethylenedinitrilotetraacetic acid
FS	fibrous sheath
kDa	kiloDaltons
mRNA	messenger ribonucleic acid
MS	mitochondrial sheath
NGS	normal goat serum
NP40	nonyl phenoxylpolyethoxylethanol
ODF	outer dense fibre(s)
PAGE	polyacrylamide gel electrophoresis
PBS	phosphate buffered saline, pH 7.7
PBST	PBS with 0.05% Tween-20
PC2	serine protease prohormone convertase 2
PMSF	phenylmethanesulphonylfluoride
PVDF	polyvinylidine difluoride

SDS	sodium dodecyl sulphate
SDS-DTT	1% SDS, 2mM DTT, 25mM Tris-HCl, pH 9
TBS	tris buffered saline, pH 7.7
TEMED	N, N, N', N' – tetramethylethylenediamine
TWBS	TBS with 0.1% Tween-20, pH 7.7
Triton-DTT	2% Triton X-100, 5mM DTT, 50mM Tris-HCl, pH 9
urea-DTT	4.5M urea, 25mM DTT, 25mM Tris-HCl, pH 9

Chapter I – Introduction

1.1 The Sperm Tail Structure

The main function of the spermatozoon flagellum is to propel it, giving it the motility required for the sperm to travel through the female reproductive tract, reach the oocyte, and penetrate the zona pellucida at fertilization. Mature mammalian sperm tails can be divided into four main structures which lie under the plasma membrane: the axoneme, the mitochondrial sheath (MS), the fibrous sheath (FS), and the outer dense fibres (ODF) [1, 2]. The tail itself can be divided into three parts: the middle piece, the principal piece, and the end piece (Figure 1). The annulus of the tail separates the middle piece from the principal piece. It is connected to the sperm head by the connecting piece.

1.1.1 The Axoneme

The axoneme consists of a central pair of microtubules surrounded by nine evenly spaced doublet microtubules in a 9+2 pattern which is reminiscent of cilia and flagella throughout the plant and animal worlds (Figure 2) [1]. Two dynein arms are attached to one subunit of each doublet which project towards the neighbouring doublet, and use chemical energy found in adenosine triphosphate (ATP) to generate a cyclic pattern of attachment and detachment which causes the adjacent microtubules to slide against one another [1, 3, 4]. Each doublet is connected to the adjacent doublets on either side by nexin, and radial spokes which join it to the central pair of microtubules [1]. Dimers of tubulin α and β make up the microtubules of the axoneme, and while a large number of axonemal accessory proteins have been found via genetic and proteomic studies in cilia

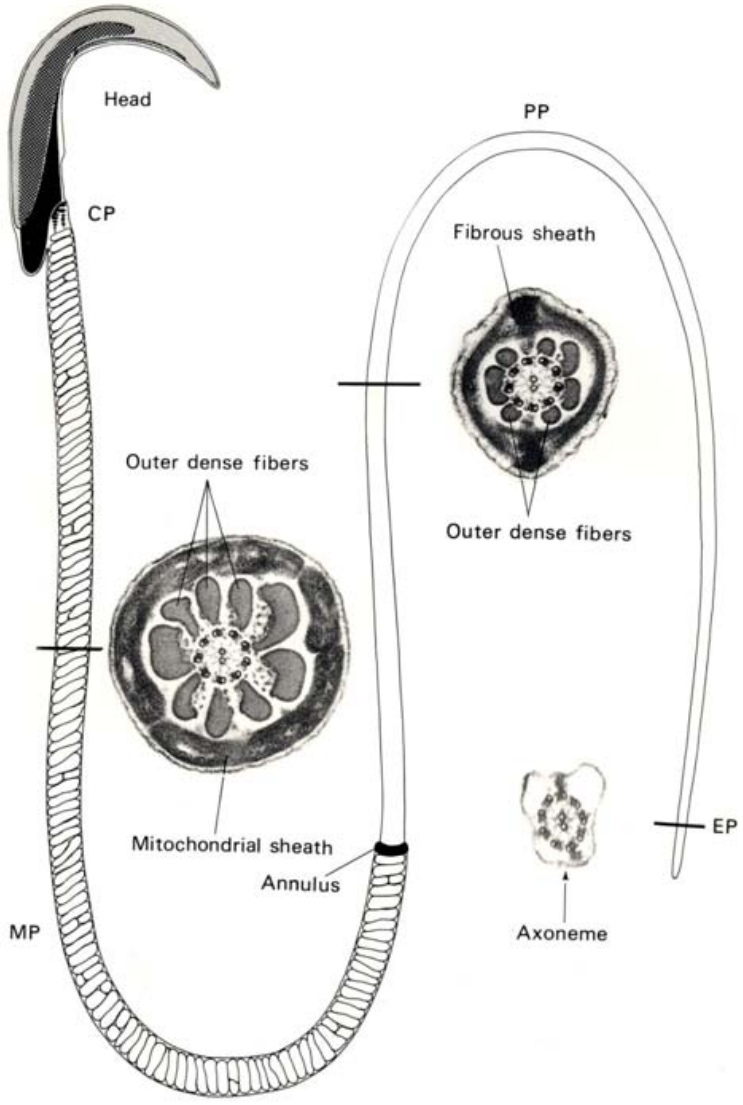

Figure 1

Diagrammatic representation of a spermatozoon showing the head, connecting piece (CP), middle piece (MP),annulus, principal piece (PP), end piece (EP), and cross sections of the MP, PP, and EP at locations indicated by the horizontal bars across the sperm tail. Outer dense fibres, the mitochondrial sheath, and the fibrous sheath are indicated in the cross sections. In the head, the acrosome is seen in light grey, the nucleus in medium grey, and the perinuclear theca in dark grey. Used with permission (Dr. Richard Oko, Department of Anatomy and Cell Biology, Queen's University, Kingston, Ontario, Canada K7L 3N6).

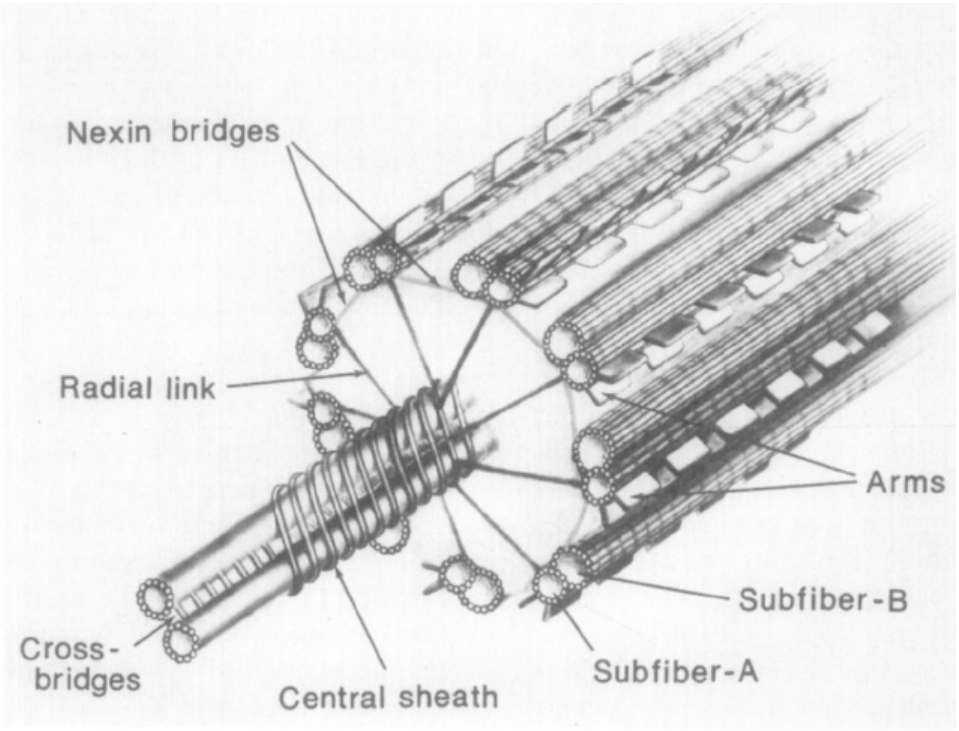

Figure 2

Diagrammatic representation of a transverse section through the tail of a spermatozoon showing the axoneme with its accessory fibres removed. Used with permission [1].

[5], sperm-specific accessory proteins have yet to be well described [6]. The axoneme extends throughout the entire length of the sperm tail.

1.1.2 The Mitochondrial Sheath

The MS is a helical arrangement of mitochondria which surround the ODF in the middle piece of the sperm tail (Figure 3). In mammals, the MS is stabilized by disulfide bonds, and is vulnerable to detachment from the sperm tail in reducing environments [7]. The need for mitochondria in the sperm tail remains mysterious because most of the energy required for sperm motility appears to be generated by glycolysis, rather than oxidative phosphorylation, suggesting that mitochondria are not required for ATP generation. In one study, mitochondrial oxygen consumption in spermatozoa lacking glyceraldehyde 3-phosphate dehydrogenase-S remain high while ATP levels drop greatly, while in another, suppression of oxidative phosphorylation has no effect on ATP levels in the presence of glucose [8, 9]. These studies demonstrate that in the presence of glucose and glycolytic enzymes, spermatozoa produce energy independent of oxidative phosphorylation and mitochondrial oxygen consumption. However, these data do not conclusively rule out a role for mitochondria in sperm energy production. It remains possible that mitochondrial energy production is turned on by a still-undiscovered trigger so as to save energy for an event such as zona pellucida penetration.

1.1.3 The Fibrous Sheath

The FS is a unique cytoskeletal structure which surrounds the axoneme and ODF under the sperm plasmalemma in the principal piece of the sperm tail (Figure 4). It is formed by circumferential, branching, anastomotic ribs that are attached to two longitudinal columns [1]. The columns are attached proximally to outer dense fibres 3

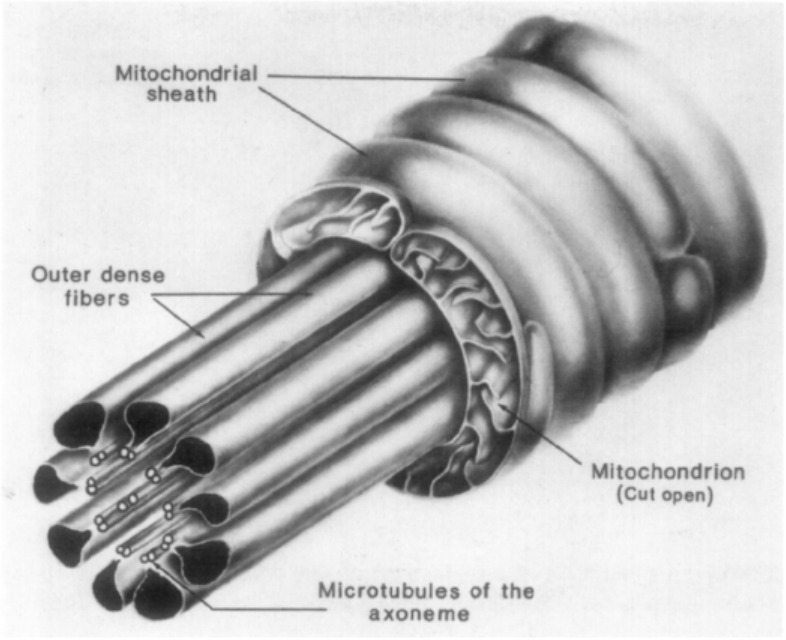

Figure 3

Diagrammatic representation of a transverse section through the middle piece of the tail of a spermatozoon, showing the mitochondrial sheath surrounding the outer dense fibres, and their association with the axonemal microtubule doublets. The overlying plasmalemma is not shown. Used with permission [1].

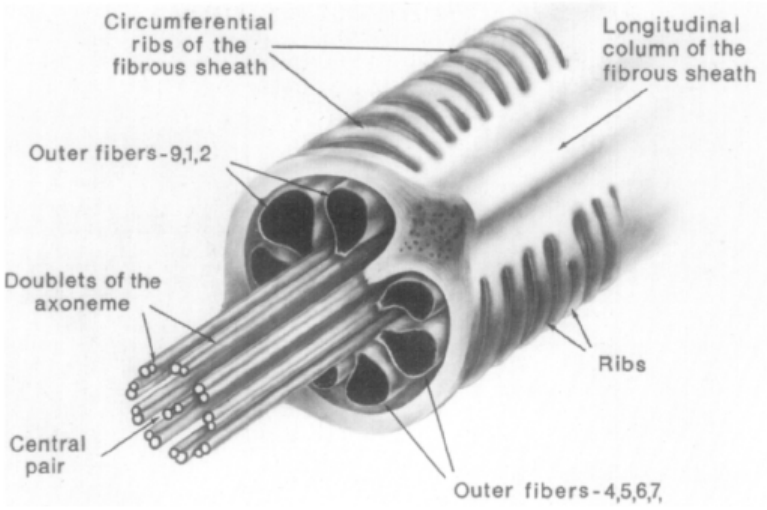

Figure 4

Diagrammatic representation of a transverse section through the principal piece of the tail of a spermatozoon, showing the fibrous sheath, with two longitudinal columns and associated ribs, and the outer dense fibres and fibrous sheath. The overlying plasmalemma is not shown. Used with permission [1].

and 8, which then replace these fibres distally through the principal piece [1, 10]. The fibrous sheath tapers and disappears distally to leave only the axoneme surrounded by the spermatozoon plasmalemma in the end piece. The FS is assembled in a distal-to-proximal manner throughout spermiogenesis, beginning with the longitudinal columns, which appear in early round spermatids and subsequently lengthen, followed by the formation of ribs [10, 11, 12].

1.1.4 The Outer Dense Fibres

In the middle piece and principal piece, the axoneme is surrounded by nine outer dense fibres. It is fixed proximally to the connecting piece and proceeds distally, with each ODF travelling superficial to an axonemal doublet [1]. It is surrounded in the middle piece by the mitochondrial sheath (Figure 3) and in the principal piece by the fibrous sheath (Figure 4). In the principal piece, outer dense fibres 3 and 8 are replaced by the longitudinal columns of the fibrous sheath, separating the ODF into two compartments with three fibres in one side and four fibres on the other. Distally in the principal piece, it tapers and disappears to leave only the axoneme surrounded by the sperm plasmalemma in the end piece. In rat spermatogenesis, the ODF begin to form in stage 7, peak by stage 14, and begin to diminish by stage 18, which correspond to stages 7, 12, and 15 in the mouse (Figure 5) , respectively, and forms in a proximal-to-distal manner, unlike the FS [12, 13].

1.1.5 The Connecting Piece and Cytoplasmic Droplet

The connecting piece consists of a capitulum which articulates with the basal plate of the spermatozoon nucleus. A vault formerly occupied by the proximal centriole is found just distal to the capitulum. Nine segmented columns extend distally from the

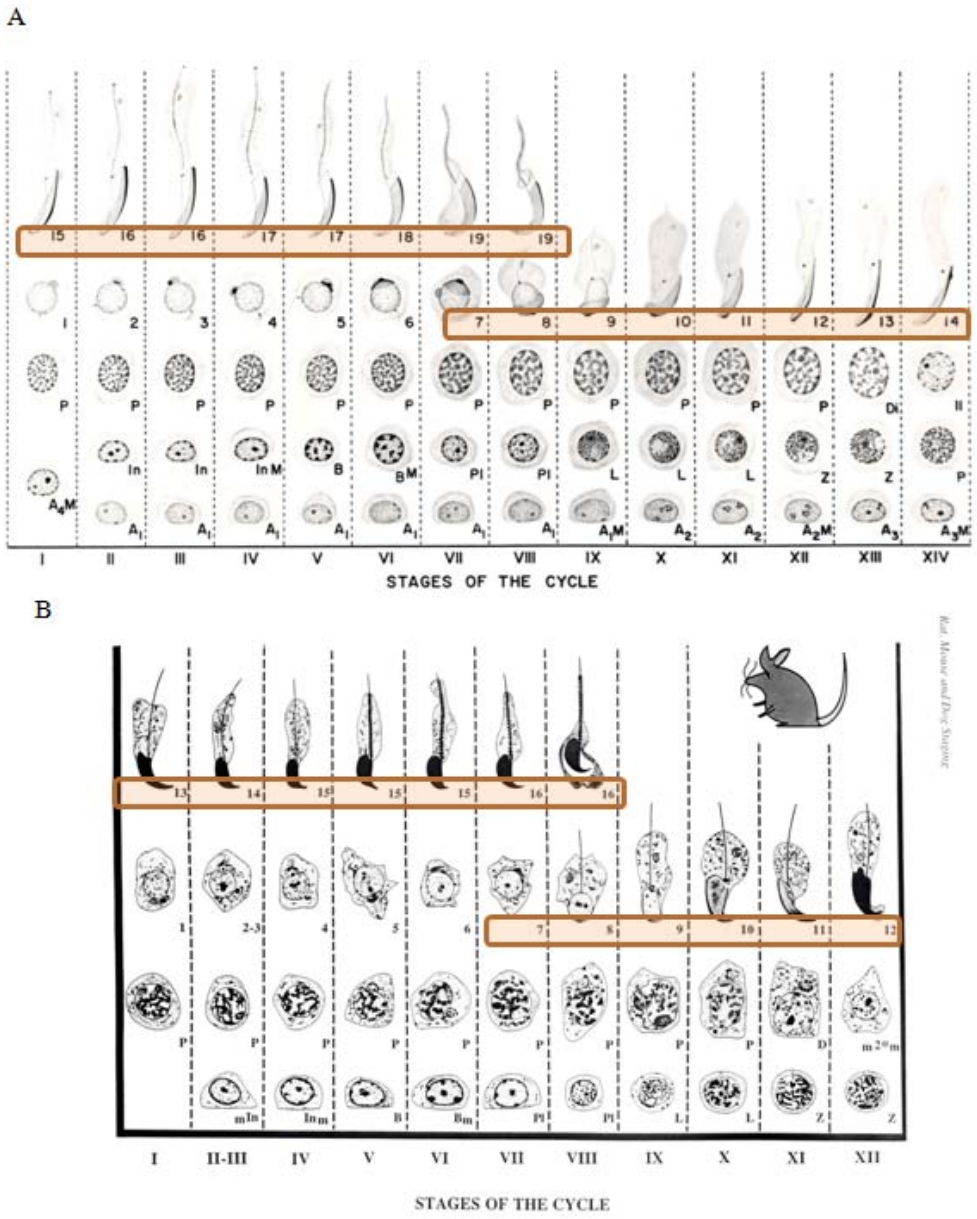

Figure 5

Diagrammatic representation of the stages of the cycle of the seminiferous epithelium in the (A) rat and (B) mouse with highlighted boxes showing the cells in which the ODF is expressed. Adapted from (A) Dym and Clermont (1970) [14] and (B) Russell et al. (1990) [15].

basal plate and are continuous with the proximal nine outer dense fibres [1]. While most of the germ cell cytoplasm is removed and phagocytosed, a cytoplasmic remnant may remain attached to a spermatozoon in this neck region following spermiation, called the cytoplasmic droplet [16]. The significance of the cytoplasmic droplet is yet unknown and contains remnants of the Golgi apparatus [17]. During epididymal transit, the cytoplasmic droplet migrates distally from its attachment to the connecting piece, through the middle piece, and detaches when it reaches the annulus.

1.2 The Sperm Head Structure

Sperm heads from different species may vary in shape, from paddle-shaped in bulls to sickle-shaped in rats and mice, but the general contents and functions between species are very similar. A basic diagram can be seen in Figure 1. Three main components of the sperm head are the nucleus, acrosome, and perinuclear theca. The sperm nucleus contains condensed chromatin, which helps streamline the spermatozoon, and is surrounded by a nuclear envelope. The acrosome is a membrane-bound secretory vesicle covering the nucleus. It is formed from the Golgi apparatus during spermiogenesis. The acrosomal matrix contains hydrolytic enzymes such as hyaluronidase and acrosin that may facilitate penetration of the zona pellucida during penetration [18]. The membrane that envelopes the acrosomal matrix is divided into the inner and outer acrosomal membranes which are continuous with each other. The acrosome can be divided into apical, principal, and equatorial segments. The acrosome reaction occurs upon initial sperm-zona binding, resulting in fusion of the outer acrosomal membrane and the plasmalemma, and the release of the acrosomal matrix; the inner acrosomal membrane and equatorial segments remain on the spermatozoon. The

perinuclear theca lies between the inner acrosomal membrane and the nuclear membrane apically, and between the plasmalemma and nuclear membrane caudally [19]. It can be divided into a subacrosomal layer, found deep to the acrosome, and a post-acrosomal sheath, found caudally between the nuclear membrane and plasmalemma [20]. Falciform spermatozoa (with a hook-shaped head) also possess a perforatorium and a ventral spur. Perinuclear theca proteins are thought to play an important role in oocyte activation, acrosome-nuclear docking, and structural stability [20, 21, 22, 23, 24, 25, 25].

1.3 Spermatogenesis

1.3.1 The Testis

Spermatogenesis is the male version of gametogenesis, and is the process by which spermatogonia develop into spermatozoa, which are the male gametes. Spermatogenesis occurs in the epithelium of the seminiferous tubules of the testes, which are highly coiled. Each end of a seminiferous tubule leads to the rete testis, which is an anastomotic system of channels found within the mediastinum of the testis. The rete testis then leads to the efferent ducts, which connect the testis to the epididymis. Between the seminiferous tubules are the interstitial spaces containing macrophages, blood and lymph vessels, and Leydig cells, which produce testosterone under regulation by hormones secreted by the anterior pituitary gland [26, 27, 28]. The seminiferous epithelium is composed of two types of cells: the spermatogenic cells and the Sertoli cells which are sustentacular cells that support them. Since they support maturing spermatogenic cells, Sertoli cells span the width of the seminiferous epithelium, extending from the base to the lumen. They secrete hormones which support and regulate maturing germ cells and phagocytose residual cytoplasm as germ cells complete

spermatogenesis. Numerous cytoplasmic extensions of the Sertoli cells allow for direct communication with developing germ cells and each other. Sertoli cells form tight junctions with each other that form the blood-testis barrier, which opens and reseals during the cycle of the seminiferous epithelium to allow maturing germ cells to migrate from the base of the seminiferous epithelium towards the lumen [29, 30].

Spermatogenesis is the process by which precursor sperm stem cells called spermatogonia develop into spermatozoa via mitotic, meiotic, and morphological changes. These changes occur in a step-wise manner causing an undifferentiated, non-polar stem cell to become a highly polarized cell with several distinct functional components. Thus, cutting a transverse section through any seminiferous tubule of the testis, would reveal that the different germ cell types do not associate with each other randomly, but according to twelve possible combinations of cellular associations called "stages" [31, 32]. The cycle of the seminiferous epithelium consists of twelve stages in the mouse (Figure 5 B) and lasts a little less than nine days [33].

Since spermatogenesis begins with spermatogonia closest to the base of the epithelium, cells towards the lumen are older, more mature, and more numerous than those towards the base. Every cell in a stage develops in a synchronous fashion, and all cells will progress over time to the next stage at the same time. This process leads to the continuous formation and release of spermatozoa into the lumen of the seminiferous tubule.

1.3.2 The First Two Phases of Spermatogenesis: Mitosis and Meiosis

Mitosis and meiosis occur in the lower two rows of cells in Figure 5 B. Spermatogonia, which are located nearest to the basal lamina of the seminiferous tubules, can undergo mitotic divisions to produce more undifferentiated spermatogonia, which ensures that the number of spermatogonia do not get depleted by replenishing their population [34]. Alternatively, they can differentiate through a series of divisions to give rise to primary spermatocytes called preleptotene spermatocytes [34]. Intercellular bridges that connect spermatogonia and spermatocytes allow for their development to occur in orderly stages, rather than in a sporadic and spontaneous way [35, 36]. The synchronicity of spermatogenesis is due to these intercellular bridges between germ cells in the same stage of development.

Primary spermatocytes then migrate towards the lumen of the seminiferous tubule, through the Sertoli-Sertoli cell junctions which form the blood-testis barrier, and undergo the first meiotic division. Primary spermatocytes are characterized as being the largest cells of the spermatogenic lineage, and give rise to secondary spermatocytes after the first meiotic division. The secondary spermatocytes then quickly undergo the second meiotic division to produce the small, haploid round spermatids [37].

1.3.3 The Third Phase of Spermatogenesis: Spermiogenesis

Spermatids then undergo biochemical and morphological changes such as elongation, condensation of the nucleus, acquisition of polarity, formation of the acrosome, formation of a flagellum, and loss of a large portion of cytoplasmic material in a process called spermiogenesis. Spermiogenesis is shown in the upper two rows of cells in Figure 5 B, where spermatids can be assigned “steps” from 1-16. Spermiogenesis can

be divided into four phases: Golgi, cap, elongation (also known as acrosomal), and maturation.

The Golgi Phase

In the Golgi phase, which begins in step 1 round spermatids (stage I, Figure 5 B) the Golgi apparatus forms small proacrosomic vesicles which are rich in hydrolytic enzymes. The small proacrosomic vesicles then fuse to form a single large acrosomic vesicle. The acrosomic vesicle associates tightly with the nuclear membrane, and thus becomes the acrosome. The early acrosome continues to receive glycoproteins via vesicles delivered from the Golgi apparatus [38].

The Cap Phase

In the cap phase, which begins in step 4 round spermatids (stage IV, Figure 5 B), the acrosome expands at the surface of the nucleus, covering half of it. The tight adhesion of the acrosome to the nuclear membrane is due to the presence of a proteinaceous substance which will later become the perinuclear theca, and covers the nucleus of spermatozoa [19].

The Elongation Phase

Elongation begins in step 8 spermatids (stage VIII, Figure 5 B), which are now called elongating, rather than round, spermatids. The nucleus begins to elongate and nuclear chromatin condenses, the acrosome flattens and elongates with the nucleus, and much of the spermatid cytoplasm is displaced caudally (towards the lumen of the seminiferous tubule). The Golgi apparatus which had been supplying acrosomal contents via small vesicles is also displaced caudally, and stops contributing contents to the

acrosome. ODF assembly and much of the formation of the sperm flagellum occur during elongation and maturation.

The Maturation Phase

Maturation begins in step 13 elongating spermatids (stage I, Figure 5 B). In the maturation phase, the acrosome takes its final form and covers the anterior part of the nucleus. Most of the spermatid cytoplasm and organelles, such as excess mitochondria and endoplasmic reticulum, are discarded in the residual body, which is reabsorbed by the Sertoli cell [17]. The remnants of the Golgi apparatus and a small amount of cytoplasm may remain on the sperm in the cytoplasmic droplet. At spermiation, spermatids are released into the lumen of the seminiferous tubule as fully formed spermatozoa.

1.4 Epididymal Maturation

1.4.1 The Epididymis

The epididymis can be divided into three main regions which are proximally to distally called the caput (head), corpus (body), and cauda (tail). It is a single tightly-coiled tube with a pseudostratified epithelial layer that connects the efferent ducts to the vas deferens, which then leads to the urethra and then to the external environment. The luminal environment in which spermatozoa mature is characterized by an ever-changing milieu of proteins due to a highly regulated process of active secretion and reabsorption by the epididymal epithelium [39, 40]. Tight regulation of epididymal luminal content is achieved by dependence on testicular androgens, testicular factors in the luminal fluid entering the epididymis, transcription factors, and spermatozoa themselves [40].

Epididymal luminal fluid is much more concentrated than testicular luminal fluid (in terms of both protein and spermatozoa concentration) because the efferent ducts reabsorb the vast majority of the volume of luminal fluids flowing from the testis before it enters the epididymis [41].

There are six cell types which can be found within the epididymal epithelium: principal cells, narrow cells, apical cells, clear cells, basal cells, and halo cells. Sixty-five to eighty percent of the cells which make up the epididymal epithelium are composed of principal cells, which are responsible for the secretion of the bulk of numerous region-specific proteins that are critical in the maturation process [40]. Narrow, apical, and clear cells are implicated in the secretion of H^+ ions which contribute to the acidification of the epididymal lumen, and intraluminal control of pH is critical for proper sperm maturation [40, 42, 43]. Narrow cells are columnar cells which extend only a small cytoplasmic extension to reach the basement membrane. Apical cells are located apically in the epididymal epithelium and do not extend to the basement membrane. Narrow cells and apical cells are found mainly in the initial segment of the epididymis [44]. Clear cells are large endocytic cells which are responsible for clearance of material from the epididymal lumen such as cytoplasmic droplets, and secreted epididymal proteins [45, 46]. Basal cells lie on the basement membrane of the epithelium and do not have contact with the lumen. They may play a role in detoxification, prevention of sperm antigen presentation to the immune system, and also closely associate with principal cells [40, 47, 48]. Lastly, halo cells are small, spherical cells which are the primary immune cells of the epididymal epithelium, and may correspond to T-lymphocytes [40, 49].

Spermatozoa which are released by the seminiferous tubule epithelium at spermiation are neither motile nor fertile [50]. Upon leaving the testis, these immature spermatozoa float into the initial segment of the epididymis after travelling through the rete testis and efferent ducts. In the epididymis, spermatozoa undergo physiological and functional maturation where they are stored until ejaculation [50, 51].

1.4.2 Epididymal Maturation

Spermatozoa contain very little cytoplasmic material after spermiation, with most cytoplasmic material extruded as the residual body before spermiation, which is then phagocytosed by the Sertoli cell. Since the spermiated spermatozoon possesses condensed chromatin which are unable to be transcripted, and no ribosomes with which to translate mRNA, maturational changes which occur during epididymal transit must be induced exclusively by factors which are present in the epididymal luminal environment and enzymes such as glycosidases and glycosyltransferases, which can be found in the luminal fluid, and are implicated in sperm maturation [52]. Changes that occur during sperm maturation in the epididymis, such as the acquisition of motility, are required for sperm to acquire the ability to fertilize the oocyte [53, 54, 55]. Intraacrosomal proteins have been shown to undergo intraacrosomal changes in localization during epididymal transit [56]. Other changes include addition/removal/modification of sperm surface proteins, deglycosylation, and the ability to undergo tyrosine phosphorylation which occurs during capacitation [57, 58, 59]. Furthermore, there must be an activation of signal transduction pathways within the spermatozoon by which interactions between the sperm surface and the epididymal luminal environment can effect changes deep within the sperm which are not in contact with the luminal environment. Epididymal maturation

is thus a highly regulated, tightly controlled process which is required for fertilization. The mechanisms for these changes remain poorly described. Specific enzymes may play a role in this process, and as such, enzyme inhibitors may play an important role in regulating enzymatic activity to ensure proper processing of proteins and signals received by the sperm.

1.5 Capacitation

Capacitation is a still-poorly defined process of further differentiation of mature spermatozoa which occurs as they travel in the female reproductive tract. These changes include further remodelling of the sperm plasmalemma, and the activation of a cyclic adenosine monophosphate (cAMP) mediated tyrosine phosphorylation signal transduction cascade. This is the final step in the maturation of spermatozoa, and results in the destabilization of the sperm head plasmalemma. As a consequence, the membrane increases permeability to calcium ions, rendering it better able to trigger the acrosome reaction, which is the exocytosis of the acrosome from the sperm head upon primary binding of the spermatozoon and oocyte. Capacitation is believed to be preceded by the removal of sperm surface inhibitory proteins called decapacitation factors which mask sperm surface receptors [60, 61, 62]. Surface receptors are then exposed to the external environment of the female reproductive tract, which then trigger capacitation. Other changes that occur during capacitation include a hyperactivated pattern of motility and increased phosphorylation of several proteins [54, 58, 63].

1.6 Cystatin-Related Epididymal Spermatogenic Protein

Cystatin-related epididymal spermatogenic (CRES) protein, also known as cystatin 8, is found in reproductive tissues and the gonadotropic cells of the anterior pituitary gland [65, 66]. There are two *Cres* mRNA splice variants which correspond to two CRES protein isoforms, which are 12- and 14 kDa in size, which can be N-link glycosylated to 17- and 19 kDa, respectively [66, 67]. Aside from localization studies, the significance of glycosylation of CRES has not yet been thoroughly explored. Glycosylation may play a role in promoting proper folding, structural stability, and proper interaction of CRES with other proteins.

It has a low sequence identity with cystatin C, a defining member of the family 2 cystatin superfamily of cysteine protease inhibitors, which act by directly competitively inhibiting its target [67]. It is considered a member of the family 2 cystatins by virtue of its conserved gene structure and colocalization with cystatin C on chromosome 2 of the mouse [67]. However, it lacks one of three consensus sites necessary for cysteine protease inhibitory activity. In mice, CRES possesses conserved C-terminal proline-tryptophan and N-terminal glycine sites necessary for cysteine protease inhibition activity, but lacks a glutamine-valine-glycine (Q-X-V-X-G) loop segment, which is the third necessary consensus site [65]. Furthermore, CRES has a poorly conserved N-terminal region, which is responsible for tight binding with cysteine proteases [67]. CRES is unable to inhibit cysteine proteases such as papain and cathepsin B, and is likely a competitive inhibitor of serine proteases [68]. Indeed, assays of enzymatic activity has demonstrated its ability to inhibit serine protease prohormone convertase 2 (PC2) *in vitro*, which processes various

prohormones into their active forms [68]. Other than a demonstrated *in vitro* association with PC2, its specific function remains a mystery.

In the testis, CRES protein has been shown to be expressed mainly during spermatid elongation and maturation, the last two phases of spermiogenesis, in stages VIII to VIII in step 8 to 16 spermatids, and has also been shown to have region-specific expression in the epididymis [69]. CRES mRNA, on the other hand, is expressed specifically during stages VII to X in step 7 to 10 spermatids [69]. CRES mRNA is also first detected in the mouse testis on postnatal age day 20, when round spermatids first appear in the seminiferous epithelium, and CRES protein first appears on day 22 when elongation begins [70]. This is not surprising, as transcription does not occur in elongating spermatids after nuclear chromatin has condensed [71]. As such, proteins required for the latter phases of spermatogenesis are translationally delayed – the required mRNA is produced earlier and stored until needed. However, CRES mRNA does not appear to be stored because as previously noted, CRES mRNA disappears from spermatids after stage X [69]. CRES protein is also found on spermatozoa. The specific expression of CRES in reproductive tissues makes it of interest to reproductive biologists.

Syntin and Cornwall demonstrated CRES localization to the acrosome of mouse spermatozoa in a 1999 study using indirect immunofluoresence, immunogold electron microscopy, and Western blot analysis [72]. In that study, indirect immunofluoresence of epididymal spermatozoa revealed fluorescent signals representing CRES that was restricted to the acrosomal region in permeabilized epididymal spermatozoa, but not membrane-intact epididymal spermatozoa [72]. Since they showed that the fluorescent signal was present only in permeabilized spermatozoa, they concluded that CRES is not associated with the sperm

surface, but is found within the acrosome. They detected no fluorescent signal distinguishable from a background signal in any other compartment of spermatozoa, including in the sperm tail. Immunogold electron microscopy performed in that study also showed gold particles localized over the acrosome, with no specific labelling found in any other structure of spermatozoa [72]. Furthermore, they analyzed acrosome-reacted cauda epididymal spermatozoa using indirect immunofluoresence and showed that CRES is released by the acrosome reaction [72]. Western blotting analysis of three fractions of acrosome reacted spermatozoa: 1) the soluble fraction after induction of the acrosome reaction, 2) the membrane-bound fraction, and 3) the remaining structures on spermatozoa, also appeared to indicate that CRES is released by the acrosome reaction [72]. Syntin and Cornwall also demonstrated different Western blot profiles of CRES proteins between caput and cauda epididymal spermatozoa, with caput spermatozoa containing both glycosylated and non-glycosylated isoforms, and cauda spermatozoa containing only the non-glycosylated isoforms [72]. In the same study, Syntin and Cornwall also performed Western blotting analysis of sequential extractions of spermatozoa. In proximal caput epididymal spermatozoa, some CRES protein was extracted with Triton X-100, but sodium dodecyl sulphate (SDS) was required to extract the majority of CRES from spermatozoa [72]. In cauda epididymal spermatozoa, SDS was insufficient for extraction of CRES protein from spermatozoa, and Laemmli buffer was required [72]. Syntin and Cornwall theorized that this might be due to a high degree of sulfhydryl cross-linking that occurs during epididymal transit.

1.7 Project Hypothesis and Objectives

The localization of proteins on spermatozoa is an important early step in determining its role as different compartments are responsible for different functions.

For example, the perinuclear theca contains proteins important for oocyte activation [21, 73], while the inner acrosomal membrane plays a role in sperm binding and penetration through the zona pellucida [75, 76]. As the role which CRES plays in reproduction remains enigmatic, determining the localization of CRES in spermatozoa is an important step in determining its function.

The late developmental expression of CRES and the harsh extraction conditions required to extract CRES from spermatozoa appears to be incompatible with the report localizing CRES to the acrosome of spermatozoa [72]. As previously discussed, the acrosome is formed in round spermatids, during the first two phases of spermiogenesis with no further Golgi contributions in elongating spermatids [37, 38, 74]. Thus, the major objective of this study was to determine the origins of CRES in the testis and its residence in mouse spermatozoa.

Due to the conflicting reports that CRES expression in the testis occurs largely in the latter stages of spermiogenesis [69] and that it is found in the acrosome [72], the approach of this study included attempts to confirm or clarify these previously published data, beginning with an immunohistochemical analysis of CRES expression in the testis. Therefore, we had two working hypotheses. In the first hypothesis, if we determine that CRES expression in the testis occurs in the latter stages of spermiogenesis, then it would likely be localized to the perinuclear theca of the sperm head or accessory structures of the sperm flagellum, as the formation of these structures are defining events in elongation and maturation. In the second hypothesis, if testicular expression begins early in spermiogenesis, then it might indeed be found in the acrosome, and it would be easily solubilised from spermatozoa by detergent extractions. We also sought to examine the

nature of CRES interaction with spermatozoa in the epididymis, where CRES has been shown be found in high levels in the luminal environment. The combined biochemical and physical fractionation, and immuno-ultrastructural approach used in this study reveals that CRES is assembled during spermiogenesis as a permanent ODF-associated protein of the sperm tail, and that CRES secreted by the caput epididymal epithelium into the luminal environment likely binds transiently to the surface of caput spermatozoa.

Chapter 2 – Materials and Methods

2.1 Animals and Sperm Collection

Male retired breeder CD1 mice were purchased from Charles River, St Constant, Quebec, housed under a 12 hour light/dark cycle, and allowed free access to food and water. Retired breeder mice were used due to their proven fertility and ability to produce spermatozoa. They were sacrificed by cervical dislocation and the epididymides were either kept whole, or cut to separate the caput and cauda, and minced in phosphate buffered saline (PBS), pH 7.4, with Complete Mini, ethylenedinitrilotetraacetic acid (EDTA) -free protease inhibitor cocktail from Roche Diagnostics, Indianapolis, Indiana, which allowed epididymal sperm to diffuse into the fluid. The fluid and tissue were filtered using 150 micron Nytex netting to separate epididymal epithelium from spermatozoa, and centrifuged at 3,000g at 4º C for 10 min, in order to obtain epididymal spermatozoa in the pellet and epididymal luminal fluid in the supernatant. Epididymal spermatozoa were then washed thoroughly by repeated resuspension in PBS followed by centrifugation in the same conditions. *Cres* -/- (knock out) and wild type epididymal mouse spermatozoa and testis were kindly donated by Dr. Gail Cornwall (Department of Cell Biology and Biochemistry, Texas Tech University, Lubbock, Texas). In brief, *Cres*-/- mice were generated through targeted disruption of the Cres gene by InGenious Targeting Laboratory, Inc (Stony Brook, NY), and were routinely genotyped using RT-PCR. Northern and western blots have demonstrated the complete lack of expression of the CRES RNA and protein.

2.2 Sonication

Phenylmethanesulphonylfluoride (PMSF) was added to epididymal spermatozoa suspended in PBS, to a dilution of 1:100, and sonicated at 44 kHz on ice for 10 seconds, 3 times, being cooled between each sonication for 30 seconds, using a Vibra-Cell sonicator, from Sonics and Materials Inc, Newtown, Connecticut. Sonicated spermatozoa were centrifuged at 4º C for 10 min at 14,000g and soluble fraction, found in the sonicated supernatant, collected. The pellet was washed three times by resuspension in PBS and centrifugation at 10,000g for 3 min at room temperature.

2.3 Isolation and Separation of Sonicated Sperm Heads and Tails

The pellet after sonication was resuspended in an 80% sucrose gradient in PBS and centrifuged at 150,000g in an angle rotor for 120 min at a temperature of 4º C to separate sonicated sperm heads and tails. Isolated heads are denser than 80% sucrose and were found on the outside edge of the centrifuge tube (towards the wall of the centrifuge), while tails are less dense than 80% sucrose, and were found on the inside edge of the centrifuge tube (towards the centre of the centrifuge). The heads and tails were separately collected and washed three times by resuspension in PBS and centrifuged at 10,000g for 3 min at room temperature. Analysis of the head and tail samples by phase microscopy indicated a sample purity of >99% for both heads and tails. Phase contrast microscopy uses variations in the refractive index of different cell structures to add contrast which would not otherwise be seen through a bright field microscope. Some structures that are either very transparent or similarly transparent to surrounding structures would not appear in high contrast under bright field, but would appear more

clearly under phase contrast. Flagella are an example of structures that appear much more clearly under phase contrast.

2.4 Extractions of Sperm Samples

Some spermatozoa were resuspended in either 0.2% Triton X-100, 1% nonyl phenoxylpolyethoxylethanol (NP40) or 2% SDS in PBS and continuously agitated overnight at 4º C. They were then centrifuged at 4º C for 10 min at 14,000g and the supernatant was collected. The pellet was washed three times by resuspension in PBS and centrifugation at 10,000g at room temperature.

Some isolated tails were resuspended in Triton-DTT (2% Triton X-100, 5mM dithiothretiol (DTT), 50mM Tris-HCl, pH 9) for 15 min and continuously agitated for 15 min at room temperature [77]. They were then centrifuged at 14,000g at 4º C for 10 min and the supernatant was collected. The pellet was washed with 50mM Tris-HCl, pH 9, twice, and then extracted again with Triton DTT for a further 15 min [77]. After repetition of the previous centrifugation and washing conditions three times, the pellet was further resuspended in either urea-DTT (4.5M urea, 25mM DTT, 25mM Tris-HCl, pH 9) or SDS-DTT (1% SDS, 2mM DTT, 25mM Tris-HCl, pH 9). The tails in SDS-DTT were extracted at room temperature for 30 min and a further 60 min, and between each extraction they were centrifuged at 14,000g at 4º C for 10 min, the extracts was collected, and they were washed by resuspension in 25mM Tris-HCl, pH 9 and centrifuged at 14,000g at 4º C for 10 min twice. The final tail pellet was washed and centrifuged in the same conditions three times, and all samples were mixed/resuspended in Laemmli buffer (with a final concentration of 2% SDS, 5% β-mercaptoethanol, 50% glycerol) [77]. The tails in urea-DTT were extracted at 4º C for 30 min, a further 90

min, and a further 180 min, and between each extraction they were centrifuged at 14,000g for 10 min at 4º C, the extract was collected, and they were washed by resuspension in 25mM Tris-HCl, pH 9 and centrifuged at 14,000g for 10 min at 4º C twice. The final tail pellet was washed and centrifuged in the same conditions three times, and all samples were mixed/resuspended in Laemmli buffer [77]. Triton-DTT has been shown to solubilise the mitochondrial sheath, SDS-DTT has been shown to solubilise the fibrous sheath, and urea-DTT has been shown to solubilise the outer dense fibres [77, 78].

2.5 Antibody Used

The antibody used in this study was kindly donated by Dr. Gail Cornwall (Department of Cell Biology and Biochemistry, Texas Tech University Health Sciences Centre, Lubbock, Texas). In brief, immune serum was raised in rabbits against C-terminally truncated recombinant mouse CRES protein 2 kDa smaller than the expected size of full-size CRES protein, and affinity purified on the same C-terminally truncated recombinant mouse CRES protein columns. This affinity purified immune serum will be referred to as "anti-CRES antibody," or simply "anti-CRES," and this was the only antibody used in this study. His-tagged CRES protein was also generously donated by Dr. Gail Cornwall (Department of Cell Biology and Biochemistry, Texas Tech University Health Sciences Centre, Lubbock, Texas) for the purposes of testing the specificity of the antibody.

2.6 Western Blot

2.6.1 Sodium Dodecyl Sulphate – Polyacrylamide Gel Electrophoresis

Samples were mixed in Laemmli buffer and boiled for 10 min by immersing tubes of samples in boiling water. Samples were loaded and run on a 4.5% stacking (4% acrylamide, 0.5M Tris-HCl pH 6.8, 0.1% SDS) and 13.5% polyacrylyamide separating gel (13.5% acrylamide, 1.5M Tris-HCl pH 8.8, and 0.1% SDS) [79]. Proteins from 10^7 whole or fractionated spermatozoa were loaded per lane. Caput and cauda epididymal tissue obtained were washed thoroughly with PBS after spermatozoa within them were collected. The tissue was homogenized, mixed in Laemmli buffer (100µL/epididymis) and boiled for 10 minutes by immersion in boiling water, and 20µL was loaded per lane. Epididymal luminal fluid in PBS (200µL of fluid was collected per epididymis) collected after centrifugation of epididymal spermatozoa which diffused out of epididymal tissues were also mixed with Laemmli buffer (1:1 ratio), and 20µL per lane was loaded. Electrophoresis was run at 110V for 110 min in Tris-glycine electrophoresis buffer (25mM Tris, 192mM glycine, 0.1% SDS).

2.6.2 Protein Transfer

Proteins which were separated by SDS-polyacrylamide gel electrophoresis (PAGE) were transferred onto polyvinylidene difluoride (PVDF) membrane. The gel and PVDF membrane were sandwiched between filter papers and sponges, soaked in transfer buffer containing 25mM Tris, 192mM glycine, and 0.01% SDS, and placed in the transfer cassette. The transfer was carried out at 250mA for 120 min on ice.

2.6.3 Blocking and Antibody Incubation

The PVDF membranes were blocked for 30 min at room temperature in 10% skim milk in PBS-T (PBS and 0.05% Tween-20). The membranes were then incubated with polyclonal affinity purified rabbit anti-mouse CRES antibody which were provided by Dr. Gail Cornwall (Texas Tech University, Lubbock, Texas) (0.4g/L) (anti-CRES), (1:1000) in 2% milk in PBS-T overnight at 4 º C. Spermatozoa from *Cres* -/- mice and anti-CRES antibody pre-incubated with recombinant CRES protein were used as negative controls. The blots were washed for five min six times in PBS-T while being continuously agitated. They were then incubated with a goat anti-rabbit IgG H+L antibody conjugated to horseradish peroxidase purchased from Vector Laboratories, Burlingame, California (1:20 000) in 2% milk in PBS-T for 3 hours at room temperature. They were again washed in PBS-T for five min six times while being continuously agitated. Afterwards they were incubated with Pierce SuperSignal peroxide and luminol/enhancer solution, from Thermo Fisher Scientific Inc, Rockford, Illinois, for six min, and exposed to X-ray film.

2.7 Immunohistochemistry

Immunolabelling was performed using an avidin-biotin-peroxidase complex (ABC) kit from Vector Laboratories. *Cres* -/- and some wild type testicular tissues were kindly donated by Dr. Gail Cornwall (Department of Cell Biology and Biochemistry, Texas Tech University Health Sciences Centre, Lubbock, Texas). Testicular and epididymal tissues were fixed in Bouin's fixative and embedded in paraffin and 5 μm sections placed on slides.

2.7.1 Rehydration

Slides were deparaffinised by washing in toluene for five min three times, hydrated using increasingly diluted ethanol solutions (100% ethanol for five min, 95% ethanol for five min), and treated to abolish endogenous peroxidase activity (70% ethanol + 1% hydrogen peroxide for five min), and residual piric acid (70% ethanol + 1% lithium carbonate for five min) [64, 80]. Slides were then further hydrated (70% ethanol for five min, 50% ethanol for five min) and treated to block free aldehyde groups (300mM glycine for five min) [64, 80]. They were then placed in 300mM sodium citrate and microwaved at 100% power for 2 min, followed by 15 min at 20% power, using a conventional 1,100W microwave from Danby Products Ltd, Guelph, Ontario. Sections were then allowed to cool to room temperature.

2.7.2 Immunolabelling and Staining

Slides were incubated with avidin blocking serum for 15 min, washed with TWBS (tris buffered saline (TBS) with 0.1% Tween-20), pH 7.7, for 5 min 4 times, and incubated with biotin blocking serum for 15 min. The slides were washed with TWBS for 5 min 4 times, blocked with 10% normal goat serum (NGS) in TBS for 15 min, and incubated in 1:60 anti-CRES antibody overnight at 4º C. Wild type mouse testis labelled with anti-CRES antibody pre-incubated with recombinant CRES protein, and the *Cres* -/- mouse testis labelled with anti-CRES antibody were used as negative controls. Slides were then rinsed with TWBS for five min four times, blocked with TBS + 10% NGS for five min, and incubated with biotinylated goat anti-rabbit IgG (1:200) for 30 min. They were then washed with TWBS for five min four times, and incubated with avidin-biotin complex (1:1) for 30 min, followed by washing with TWBS for five min four times.

The slides were then incubated in a 0.03% hydrogen peroxide, 0.1M imidazole, and 0.05% diaminobenzidine tetrahydrochloride (DAB) solution in TBS pH 7.5 for 8-10 min, washed with deionized water for five min twice, then tap water for five minutes, and counterstained in 0.1% methylene blue for one hour. The slides were then washed with tap water for 5 min and deionized water for 2 min twice.

2.7.3 Dehydration

This was followed by dehydration with increasingly concentrated ethanol solutions (50%, 70%, 95%, and 100% ethanol, and 1:1 toluene:ethanol for up to 1 min each, depending on the level of counterstain on the sections), clearance with toluene, and then the slides were mounted on a slide using Permount slide mounting fluid (Fischer Chemicals, Fairlawn, New Jersey) [64].

Analysis of seminiferous tubule staging was performed using criteria used by Russell *et al.* using a light microscope [15].

2.8 Immunogold Electron Microscopy

Spermatozoa were fixed in 4% paraformaldehyde and 0.8% glutaraldehyde, embedded in LR white (Canemco Inc, St Laurens, Quebec), cut into ultrathin sections and mounted on formavar coated nickel grids. All solvents and solutions were double-filtered before use with P8 Fisher brand filter paper, except for the antibody. Grids were floated tissue-side down on the various solutions. Grids were first floated on a drop of deionized water to wet them before being blocked with 5% NGS in TBS, pH 8, at room temperature. They were then incubated with anti-CRES antibody overnight at 4º C. They were then washed in TWBS (TBS with 0.1% Tween-20, pH 8) for five min five

times, followed by blocking with 5% NGS in TBS, pH 8, for 15 min. Spermatozoa on grids incubated with normal rabbit serum and and with immune serum affinity purified on proteins unrelated to CRES, rather than anti-CRES antibody, were used as negative controls. They were then incubated in 10 nm gold particle-conjugated goat anti-rabbit IgG (1:20 in TBS, pH 8) for 2 hours at room temperature, before being washed with TWBS, pH 8, for five min three times, and deionized water for five min twice, and then allowed to dry. The sections were then counterstained with uranyl acetate (1:2 of 4% uranyl acetate in deionized water:ethanol) for two min and lead citrate (0.35% lead citrate in deionized water, pH 12), washed with deionized water by dipping into vials four times, and then dried. Photographs were taken using a Hitachi 7000 transmission electron microscope.

Chapter 3 – Results

3.1 CRES expression in the mouse testis

Spermatogenesis proceeds in a step-wise manner, in which germ cells develop several distinct functional components in a highly temporally regulated way. Thus, we performed an immunohistochemical analysis of mouse testes via the immunoperoxidase reaction to confirm the stages of spermatogenesis when CRES expression begins and peaks. By comparing which components of spermatozoa are developing while CRES is being expressed, this investigation could narrow its scope.

Comparison of anti-CRES immunoperoxidase stained wild type and *Cres* -/- mouse testes confirmed a previous study [91] that CRES expression occurs mainly in elongating spermatids (Figure 6). CRES first appears in the cytoplasm of late round to early elongating spermatids in steps 7 and 8, (stages VII-VIII, Figure 7 A, B and Figure 8 E, F) intensifies during steps 9-12 (stages IX-XII, Figure 7 C, D, E, F), reaches a peak in steps 13 to 15 (stages I-V, Figure 8 A, B, C, D) and diminishes in steps 15 to 16 (stages VI-VIII, Figure 7 A, B and Figure 8 E, F), just before spermiation. CRES is not found in the acrosome of round or elongated spermatids. Pachytene spermatocytes and other non-spermatid cells the seminiferous epithelium are also clearly unstained by the immunoperoxidase reaction. Unstained heads of elongating spermatids, which appear blue, can be clearly seen in the seminiferous epithelium in Figure 7 and Figure 8. Also in Figure 8 F, initial CRES labelling can be seen beginning in step 7 late round spermatids. During the peak of CRES expression, the spermatid cytoplasm can be seen intensely stained in Figure 8 A, B, C, and D. Sections of *Cres* -/- testes incubated with anti-

Figure 6

Immunohistochemical analysis of CRES expression in spermatogenesis in the seminiferous tubules. Scale bars in all figures represents 20 μm. ES = elongating spermatids, RS = round spermatids, T = spermatid tails. Wild type testes (A) and *Cres* -/- testes (B) were stained with anti-CRES antibody as described in Chapter 2, Materials and Methods, and photographed. Sections (A) and (B) were kindly donated for staining by Dr. Gail Cornwall (Department of Cell Biology and Biochemistry, Texas Tech University Health Sciences Centre, Lubbock, Texas). Spermatid tails suspended in the seminiferous tubule epithelium are visibly stained in (A). Generally, little staining is seen in round spearmatids. Much of the staining is seen in elongating spermatids, which are intensely stained, seen (A). No staining is seen in (B), demonstrating the specificity of the antibody.

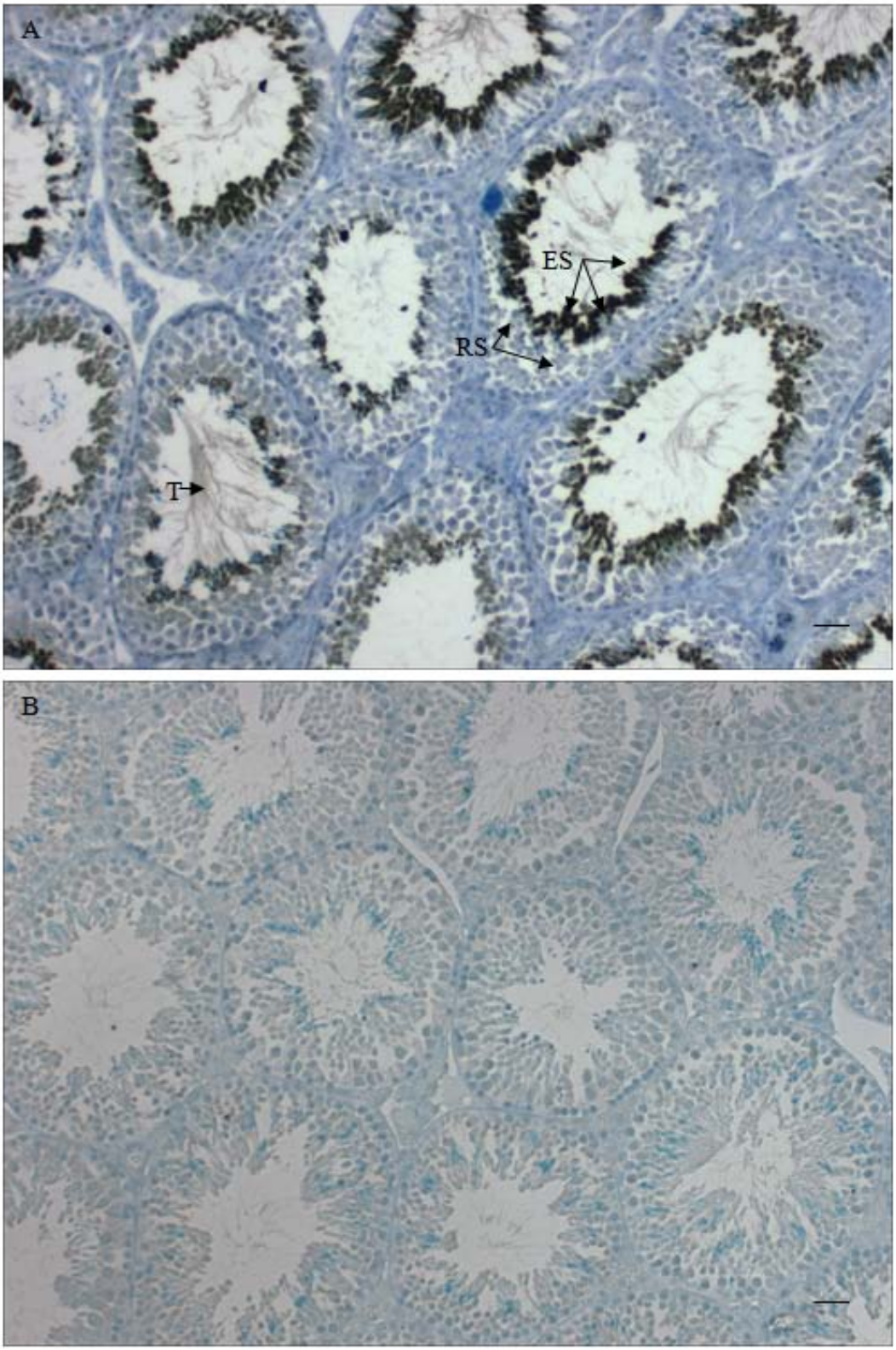
A
ES
RS
T
B

Figure 7

Developmental analysis of CRES expression in the seminiferous tubules, examined via the immunoperoxidase reaction. H = elongating spermatid heads, RB = residual bodies, RS = round spermatids, P = pachytene spermatocyte, asterisks (*) = spermatid cytoplasm, and scale bars in all figures represent 20 μm. Sections of mouse testes were stained with anti-CRES antibody as described in Chapter 2, Materials and Methods, and photographed.

A, B – A stage VIII seminiferous tubule is seen in (A), with (B) showing the seminiferous epithelium with increased magnification. CRES expression begins in step 8 late round spermatids seen in (B). Residual bodies can be seen clearly stained, while late elongating step 16 spermatid heads are seen unstained, seen in (B). The cytoplasm of step 8 round spermatids is shows slight staining in (B) and is indicative of the beginning of CRES expression. Spermatid tails suspended in the lumen are also visibly stained in (A) and (B).

C, D – A stage IX seminiferous tubule is seen in (C), with (D) showing the seminiferous epithelium with increased magnification. Clearly shown in (D), staining of the elongating spermatid cytoplasm increases in step 9 elongating spermatids from step 8 round elongating spermatids, while the heads remain unstained. Spermatid tails visibly stained in the lumen are seen in (C).

E, F – A stage X seminiferous tubule is seen in (E), with (F) showing the seminiferous epithelium with increased magnification. Clearly shown in (F), staining of the elongating spermatid cytoplasm increases in step 10 elongating spermatids, while the heads remain unstained. Pachytene spermatocytes are also seen unstained in (F). Spermatid tails visibly stained in the lumen are seen in (E).

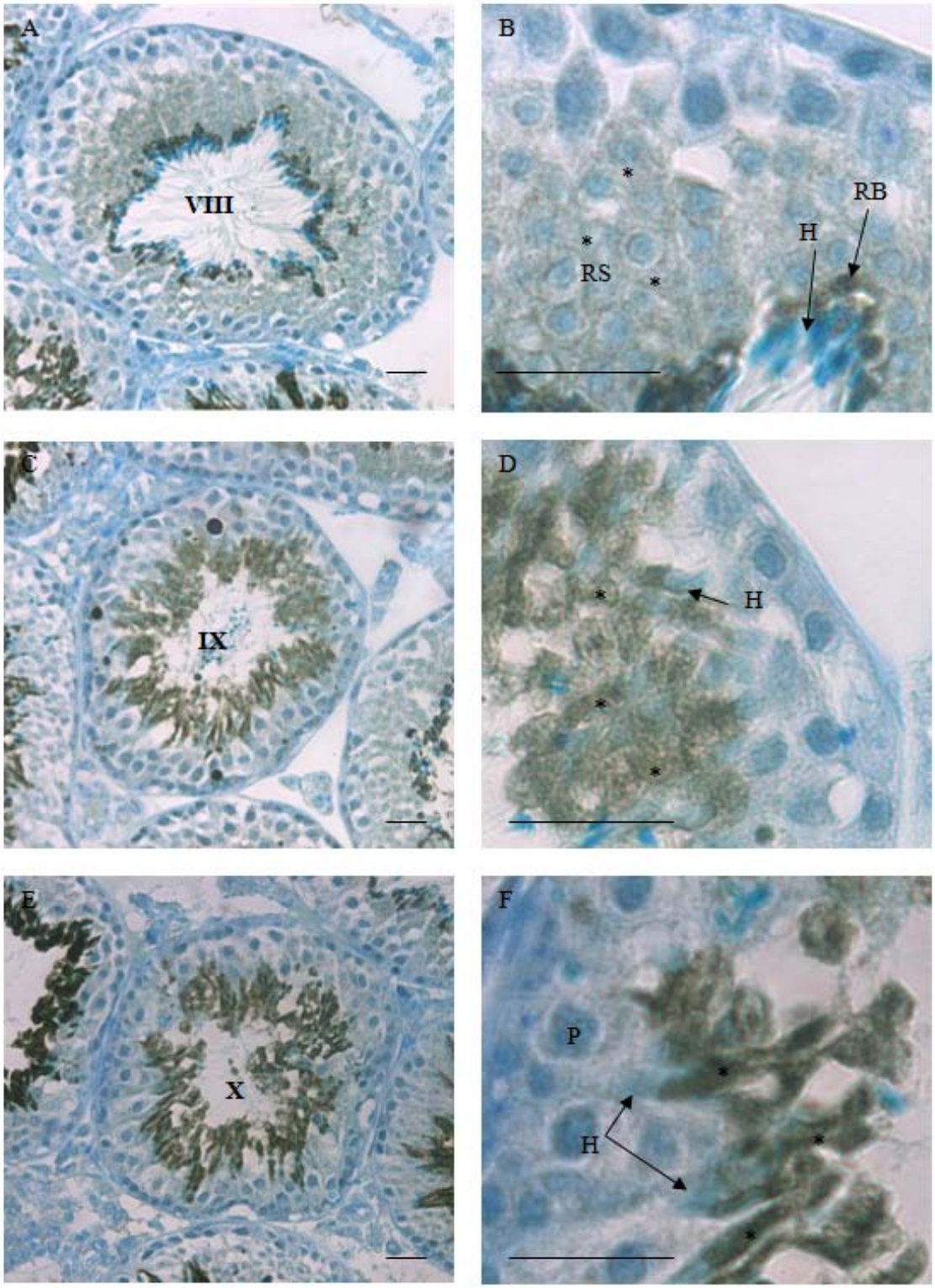
A
VIII
B
RB
H
RS
C
IX
D
H
E
X
F
P
H

Figure 8

Developmental analysis of CRES expression in the seminiferous tubules, examined via the immunoperoxidase reaction. H = elongating spermatid heads, RB = residual bodies, RS = round spermatids, asterisks (*) = spermatid cytoplasm, and scale bars in all figures represent 20 μm. Sections of mouse testes were stained with anti-CRES antibody as described in Chapter 2, Materials and Methods, and photographed.

A, B – A stage XII-I seminiferous tubule is seen in (A), with (B) showing the seminiferous epithelium with increased magnification. Clearly shown in (B), staining of the elongating spermatid cytoplasm peaks in step 12 elongating spermatids, while the heads remain unstained. Spermatid tails visibly stained in the lumen are seen in (A).

C, D – A stage IV-V seminiferous tubule is seen in (C), with (D) showing the seminiferous epithelium with increased magnification. Clearly shown in (D), staining of the elongating spermatid cytoplasm continues to peak in step 15 elongating spermatids, while the heads remain unstained. Spermatid tails visibly stained in the lumen are seen in (C).

E, F – A stage VII seminiferous tubule is seen in (E), with (F) showing the seminiferous epithelium with increased magnification. Clearly shown in (F), staining of the elongating spermatid cytoplasm diminishes in step 16 elongating spermatids, while the heads remain unstained. Late step 7 round spermatids are also seen in (F) with some very light staining in the cytoplasm. Spermatid tails visibly stained in the lumen are seen in (E).

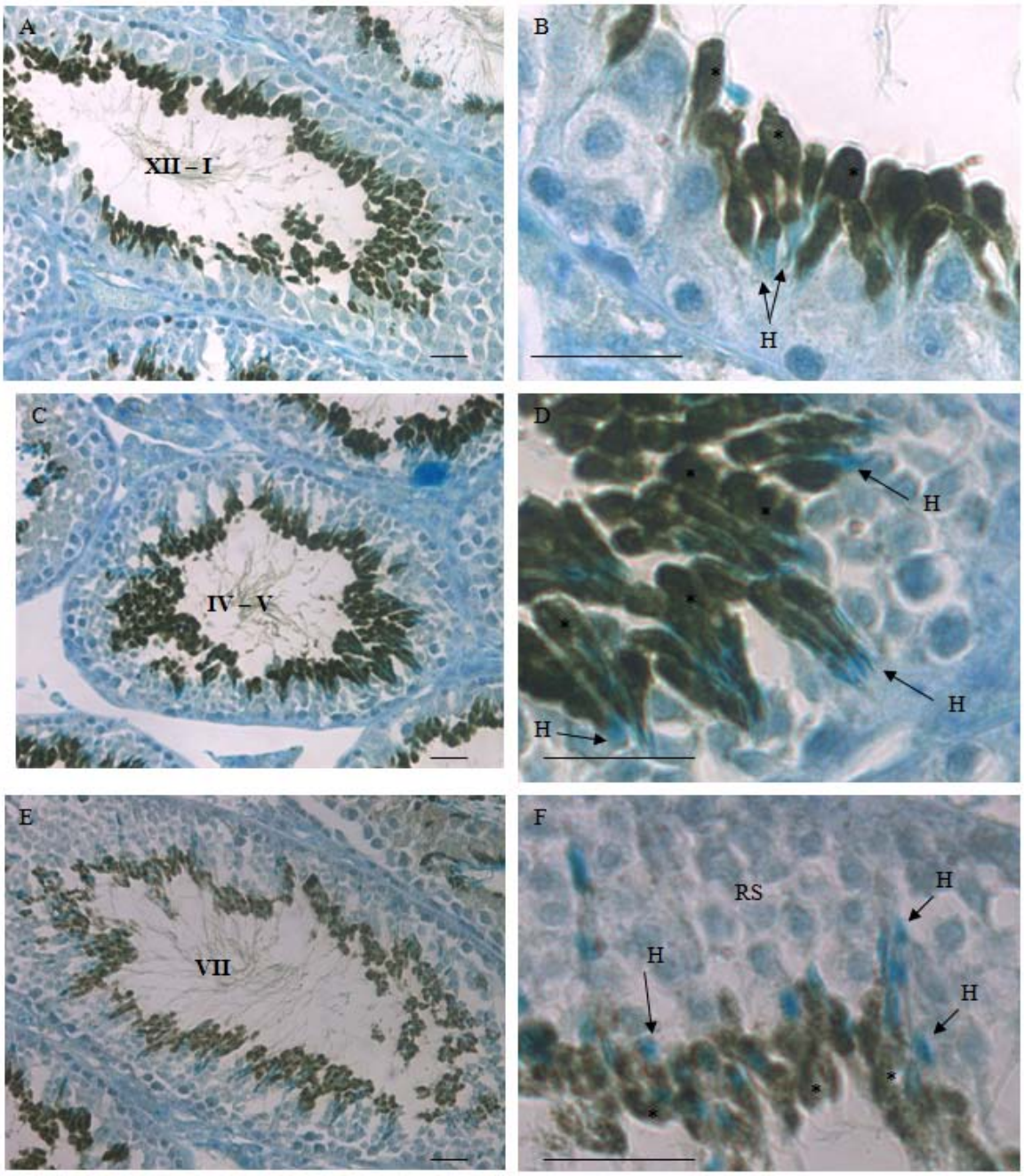
A
XII – I
B
H
C
IV – V
D
H
H
H
E
VII
F
RS
H
H
H

CRES antibody did not reveal labelling, which demonstrates the specificity of the antibody (Figure 6 B). Sections of mouse testes stained with anti-CRES pre-incubated with recombinant CRES protein also did not reveal labelling. Most importantly, throughout Figure 7 and Figure 8, spermatid tails seen suspended in the lumen of the seminiferous tubule appear to be intensely stained, indicating that CRES may be present in a component of the sperm flagellum.

3.2 CRES resides in isolated sperm tails

3.2.1 Western blots of isolated tails and extractions show CRES is present in the sperm tail

Because CRES immunoreactivity was associated with the developing sperm tail during the elongating and maturation phases of spermiogenesis, immunblotting was used to explore whether CRES was associated with the tail fraction of spermatozoa. Spermatozoa from the cauda epididymis were chosen for examination as they represent spermatozoa that have finished the process of epididymal maturation; spermatozoa from the rest of the epididymis have yet to complete the process of epididymal maturation. It is cauda epididymal spermatozoa that are stored until ejaculated, and consequently fertilize the oocyte. Comparison of immunoblotting reactivity with anti-CRES between whole wild type and *Cres* -/- cauda spermatozoa revealed one specific CRES reacting protein band at 14 kDa and an unrelated band at 66 kDa (Figure 9 A; also see [65, 72]). The 66 kDa band must be unrelated to CRES because if the *Cres* gene has been knocked out, no CRES protein should be able to be produced, yet the 66 kDa band is present in *Cres* -/- cauda epididymal spermatozoa.

Figure 9

A – Western blot analysis of 3 x 10^6 cauda epididymal spermatozoa from (1) *Cres* wild type and (2) *Cres* -/- mice labelled with anti-CRES. A 66 kDa immunoreactive band present in *Cres* +/+ spermatozoa remains present in *Cres* -/- spermatozoa (unpublished data from Dr. Gail Cornwall, Department of Cell Biology and Biochemistry, Texas Tech University, Lubbock, Texas).

B – Western blot analysis of sequential extractions of isolated sperm tails using anti-CRES antibody. 1 x 10^7 sperm tails were sequentially extracted with (1) Triton-DTT for 15 minutes. After extraction, the suspension was centrifuged, and the pellet was obtained and further extracted by resuspension in (2) Triton-DTT for a further 15 minutes (Figure 10 A shows electron micrograph of anti-CRES labelled Triton-DTT extracted tails). After extraction, the suspension was centrifuged, and the pellet was obtained and further extracted by resuspension in (3) urea-DTT for a further 30 minutes. After extraction, the suspension was centrifuged, and the pellet was obtained and further extracted by resuspension in (4) urea-DTT for a further 90 minutes. After extraction, the suspension was centrifuged, and the pellet was obtained and further extracted by resuspension in (5) urea-DTT for a further 180 minutes. After extraction, the suspension was centrifuged, and (6) the pellet after sequential extractions was mixed in Laemmli buffer, and boiled.

C – Western blot analysis of sequential extractions of isolated sperm tails using anti-CRES antibody. 1 x 10^7 sperm tails were sequentially extracted with (1) Triton-DTT for 15 minutes. After extraction, the suspension was centrifuged, and the pellet was obtained and further extracted by resuspension in (2) Triton-DTT for a further 15 minutes. After extraction, the suspension was centrifuged, and the pellet was obtained and further extracted by resuspension in (3) SDS-DTT for a further 30 minutes. After extraction, the suspension was centrifuged, and the pellet was obtained and further extracted by resuspension in (4) SDS-DTT for a further 60 minutes, and (5) the pellet after sequential extractions was mixed in Laemmli buffer, and boiled.

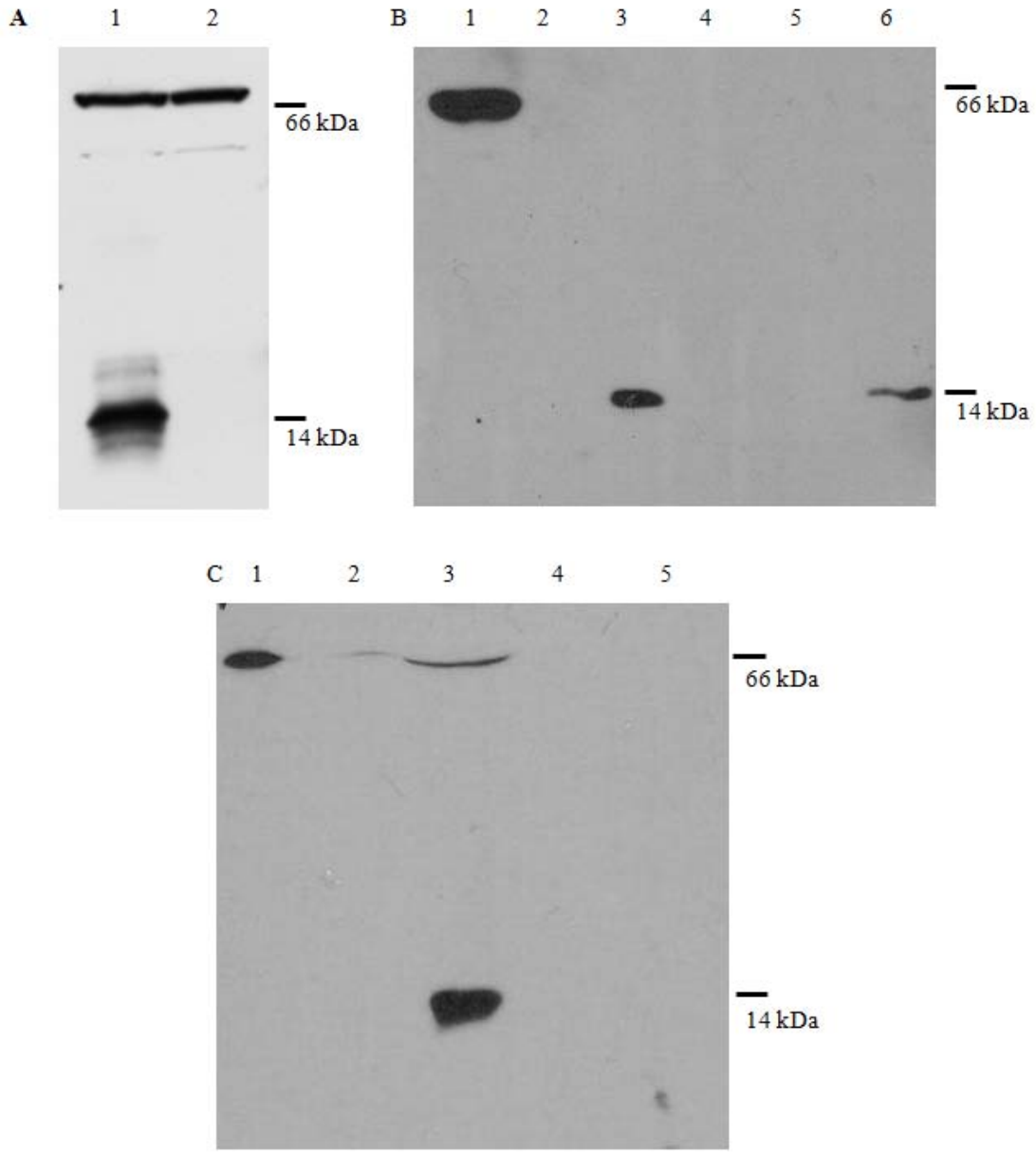
A
1
2
66 kDa
14 kDa
B
1
2
3
4
5
6
66 kDa
14 kDa
C
1
2
3
4
5
66 kDa
14 kDa

Sequential extractions of the isolated tail were performed with increasingly harsh denaturants to elucidate the nature of CRES association. The 66 kDa band was extracted into the soluble fraction after a 15 minute incubation with Triton-DTT (Figure 9 B), proven to almost denude the mid-piece of the mitochondrial sheath [77, 78] and confirmed in this study by electron microscopy (Figure 10 A). After a second 15 minute incubation with Triton-DTT (for a total Triton-DTT incubation time of 30 minutes), further incubation of the washed Triton-DTT insoluble tail pellet in harsh protein solubilising conditions (urea-DTT or SDS-DTT) was effective in extracting the specific 14 kDa band (Figure 9 B, C). This suggests that CRES is both ionically and covalently bound to one of the two accessory tail components – the ODF or FS – remaining after Triton-DTT extraction. Little 14 kDa CRES remained in the final pellet after either SD-DTT or urea-DTT extractions.

3.2.2 Immunogold electron microscopy shows CRES is associated with ODF

An ultrastructural study of Triton-DTT extracted isolated tails was then performed to further elucidate which accessory tail component CRES may be associated with. Immunogold labelling of cauda epididymal spermatozoa with anti-CRES revealed labelling over both the mitochondrial sheath and the ODF (Figure 10 B). Extraction of isolated sperm tails with Triton-DTT solubilised the mitochondrial sheath but retained the ODF and FS (Figure 10 A). Removal of the mitochondrial sheath was coincident with the extraction of the anti-CRES 66 kDa cross-reacting protein (Figure 9), suggesting that the unrelated 66 kDa protein which cross-reacts with anti-CRES is found in the mitochondrial sheath. After this extraction step, the immunogold labelling was restricted

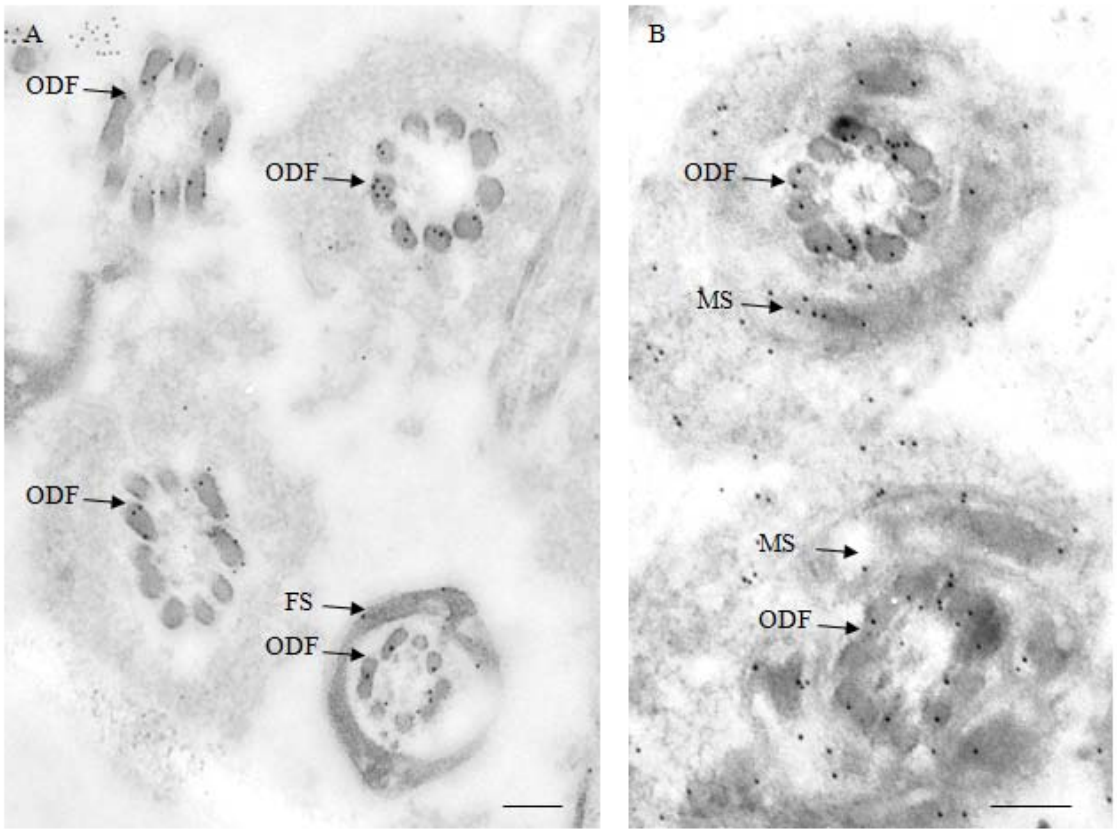

Figure 10

ODF=Outer dense fibres, FS = fibrous sheath, MS = mitochondrial sheath. Scale bars in all figures represent 0.2 μm.

A – Electron micrograph showing Triton-DTT extracted tails with the mitochondrial sheath partially removed and incubated with 1:20 polyclonal affinity purified rabbit anti-mouse CRES antibody. CRES labelling is seen specifically over the ODF.

B – Electron micrograph showing isolated tails before extraction with Triton-DTT, incubated with anti-CRES antibody. Labelling can be seen over the ODF and in the mitochondrial sheath.

to the ODF, coincident with retention of the 14 kDa immunoreactive band, which is presumably CRES.

Ultrathin sections of testicular spermatids and cauda epididymal spermatozoa were cut and immunogold labelling was performed to confirm that CRES is associated with ODF during spermatogenesis and throughout epididymal transit. This investigation revealed that CRES is associated with the ODFs in testicular spermatids (Figure 11, Figure 12, Figure 13). No immunogold label can be seen in the structures of the sperm head, including the nucleus and the acrosome (Figure 11, Figure 12). Some gold particles can also be found in the connecting piece (Figure 12). This is not unexpected as the connecting piece and ODF are continuous with each other [1]. The residual body, which contains the excess extruded cytoplasm of spermatids, is also positively labelled (Figure 13), indicating that excess CRES is produced in the maturing spermatid which is phagocytosed by the Sertoli cell. The pattern of gold labelling on cauda epididymal spermatozoa is very similar to that found in testicular spermatozoa. The immunogold label can be seen in the connecting piece, as well as strongly concentrated over the ODF, with some particles found in the MS (Figure 14). Little to no gold particles can be seen in the nucleus, acrosome, and other structures of the sperm head (Figure 15). Immunogold labelling of ultrathin sections of spermatids and spermatozoa with normal rabbit serum or immune serum affinity purified on non-CRES protein as controls did not label the ODF. Immunogold labelling of sections which were not incubated with a primary antibody also did not label the ODF. The presence of ODF-associated CRES from the testis to the cauda epididymis suggests that it is not degraded during epididymal transit.

Figure 11
Electron micrograph showing heads and a tail from testicular spermatids incubated with anti-CRES antibody. ODF = outer dense fibres, MS = mitochondrial sheath, Nu = nucleus, AS = apical segment of the acrosome, ES = equatorial segment of the acrosome, PAS = post-acrosomal sheath of the perinuclear theca, VS = ventral spur of the perinuclear theca, and P = perforatoriumof the perinuclear theca. Scale bar represents 0.2 µm. Gold particles can be clearly seen concentrated over the ODF. No specific concentrations of gold particles can be seen in any of the structures of the sperm head.

Figure 12

Electron micrograph showing a head and tails from testicular spermatids incubated with anti-CRES antibody. ODF = outer dense fibres, MS = mitochondrial sheath, FS = fibrous sheath, Nu = nucleus, CP = connecting piece. Scale bar represents 0.2 μm. As in

Figure **11**, gold particles can be clearly seen concentrated over the ODF, and no specific concentrations of gold particles can be seen in any of the structures of the sperm head. The connecting piece is also seen visibly labelled.

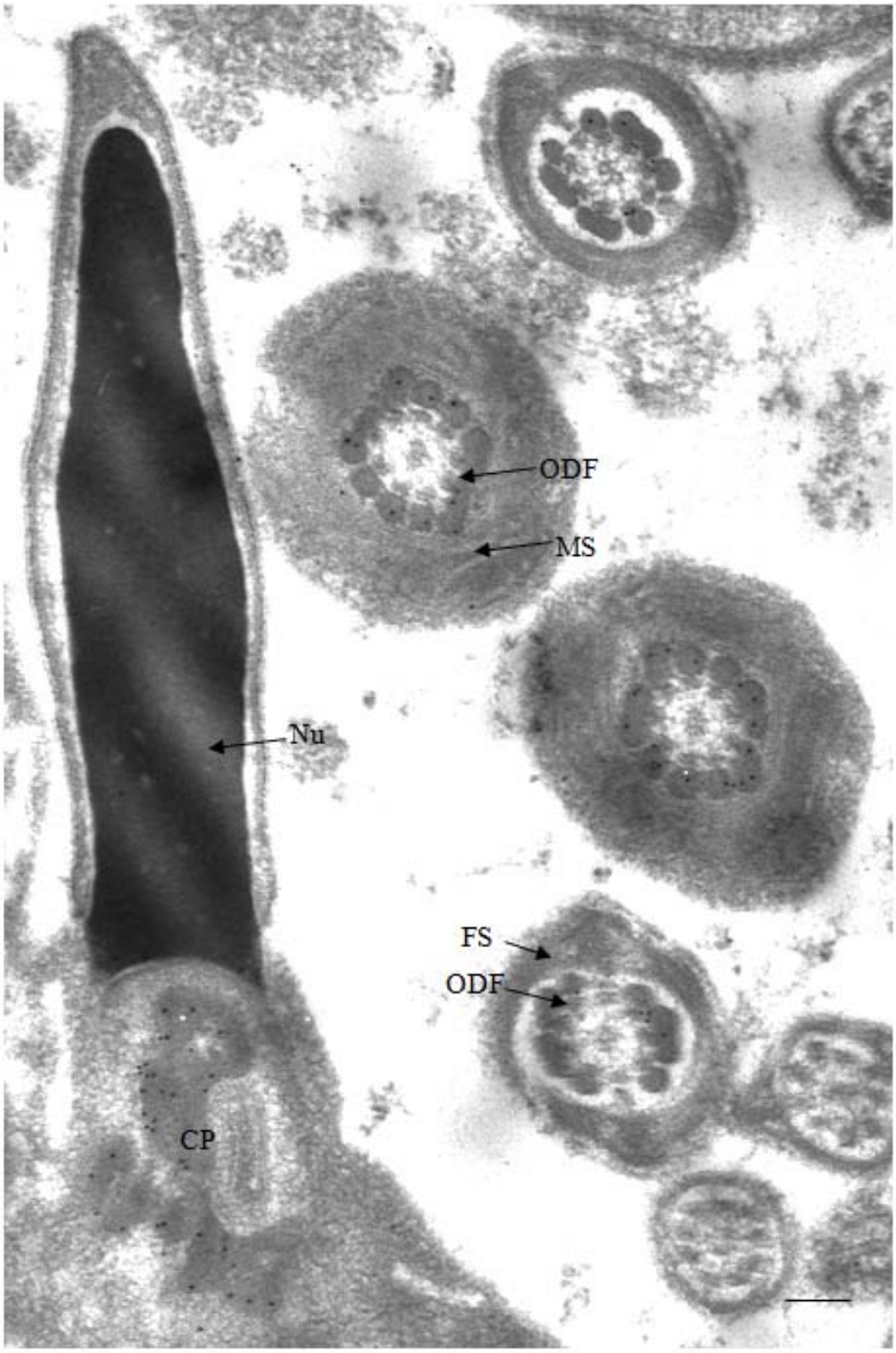
ODF
MS
Nu
FS
ODF
CP

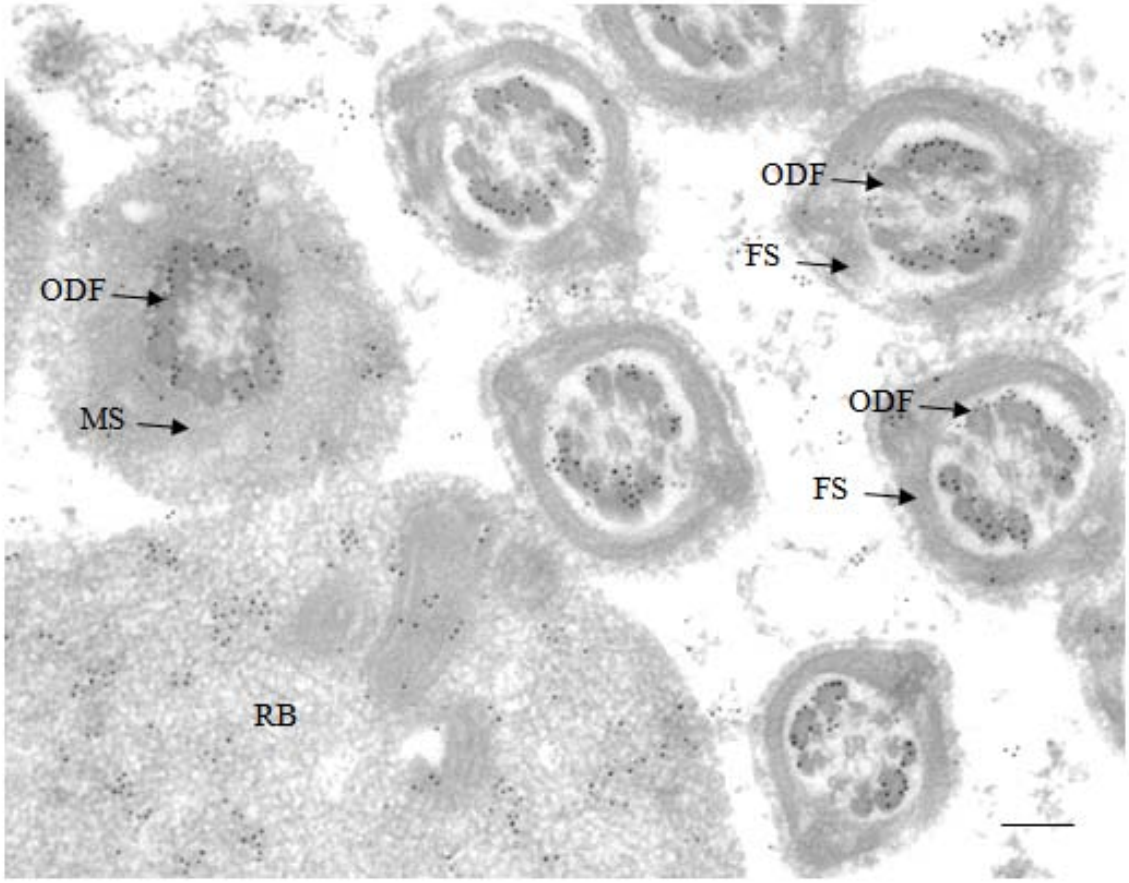

Figure 13

Electron micrograph showing tails and a residual body from testicular spermatids incubated with anti-CRES antibody. ODF = outer dense fibres, MS = mitochondrial sheath, FS = fibrous sheath, and RB = residual body. Scale bar represents 0.2 µm. Gold particles can be clearly seen concentrated over the ODF in both the middle piece and principal piece of the sperm tail. The residual body is also seen visibly labelled.

Figure 14

Electron micrograph showing tails from cauda epididymal spermatozoa incubated with anti-CRES antibody. ODF = outer dense fibres, and MS = mitochondrial sheath. Scale bars in all figures represent 0.2 μm. Gold particles can be seen concentrated over the outer dense fibres in both (A) and (B).

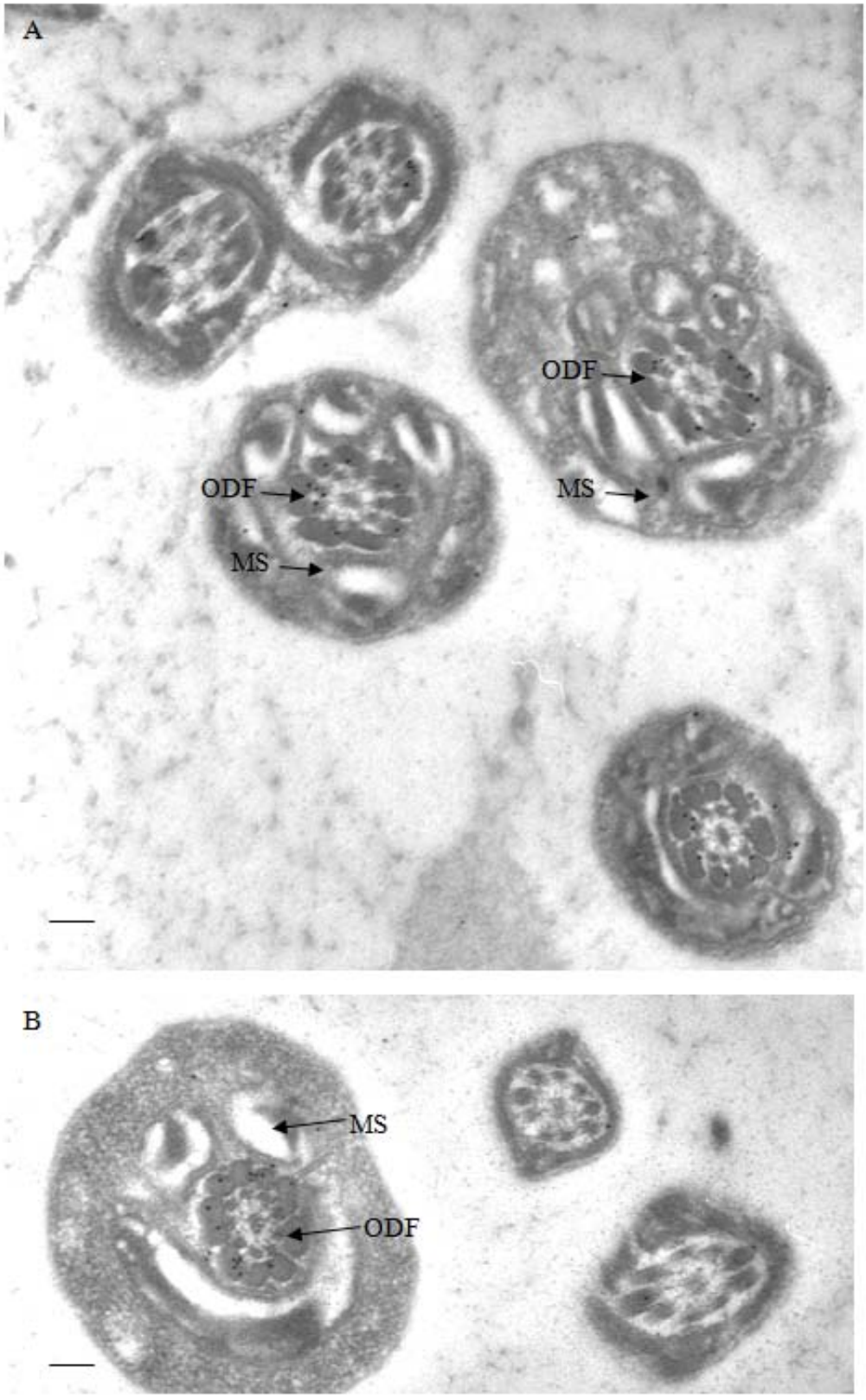
A
ODF
MS
ODF
MS
B
MS
ODF

Figure 15

Electron micrograph showing a head of a cauda epididymal spermatozoon incubated with anti-CRES antibody. CP = connecting piece, AS = apical segment of the acrosome, ES = equatorial segment of the acrosome, P = perforatorium of the perinuclear theca, PAS = post-acrosomal sheath of the perinuclear theca, and Nu = nucleus. Scale bars in all figures represent 0.2 μm. Gold particles can be seen concentrated over the connecting piece. No specific concentrations of gold particles can be seen in any of the structures of the sperm head.

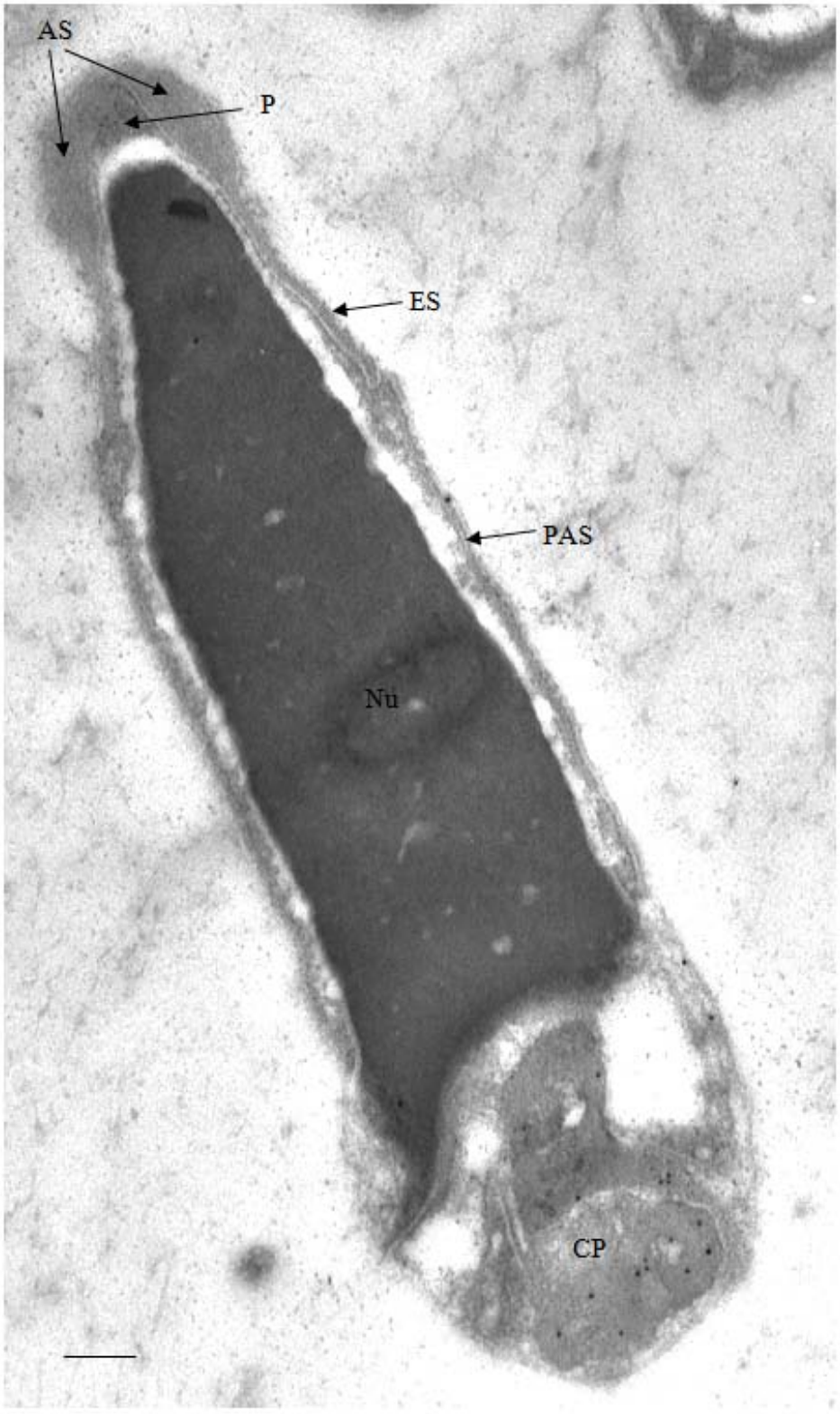
AS
P
ES
PAS
Nu
CP

3.3 CRES is expressed in the epididymis and transiently associates with the sperm surface

3.3.1 Immunoperoxidase reaction reveals CRES is secreted by the principal cells of the initial segment

It has been previously shown that CRES is expressed in principal cells of the proximal caput epididymis [69]. Thus, another objective of this study was to determine if epididymal secreted CRES associated with the sperm surface during epididymal transit. Modifications of the sperm surface during transit include addition, removal, and modification of surface proteins, and it is possible that CRES might play a role in this process. As the results of this present study are leading to different conclusions than previously published studies, we performed an immunohistochemical analysis of the epididymis to confirm past findings.

Immunoperoxidase staining using anti-CRES confirmed that CRES is expressed in the caput but in addition showed that its expression is restricted to the principal cells of the initial segment (Figure 16 A). The immunostaining was most intense in the supranuclear region of the principal cells, indicative of labelling in the Golgi apparatus (Figure 16 B, inset). Since Golgi apparatuses play an important role in glycoprotein synthesis and exocytosis, this suggests that CRES is indeed secreted by these principal cells into the epididymal luminal environment. The apical cytoplasm and luminal surface of the initial segment epithelium (Figure 16 A, B) were also strongly reactive, and further indicative of CRES secretion.

Figure 16

CRES protein localization in the epididymis as visualized by the immunoperoxidase reaction. Nu = nuclei, G = Golgi apparatus, scale bars in (A)and (E) represent 100 μm, while scale bars in (B), (C), (D), and (F) represent 50 μm. (A) shows a wider view of the initial segment, and the proximal and mid caput epididymis, and the locations of (B) and (C) are indicated by (b) and (c), respectively. (B) shows a more magnified view of the initial segment showing strong labelling of the supranuclear Golgi apparatus (indicated by arrows) of the principal cells of the epididymal epithelium, with an inset of a tissue section with more methlyene blue counterstain indicating nuclei and the Golgi apparatus, (C) shows the caput epithelium slightly distal from (B) where the supranuclear Golgi apparatus labelling of principal cells have disappeared and the clear cells of the epididymal epithelium are positively stained with CRES labelling (indicated by arrows), (D) shows the caput epididymis distal from (C) where there is no longer CRES labelling in the epididymal epithelium, (E) shows the cauda epididymis, and (F) shows a more magnified view of the cauda showing little to no CRES labelling in the epididymal epithelium.

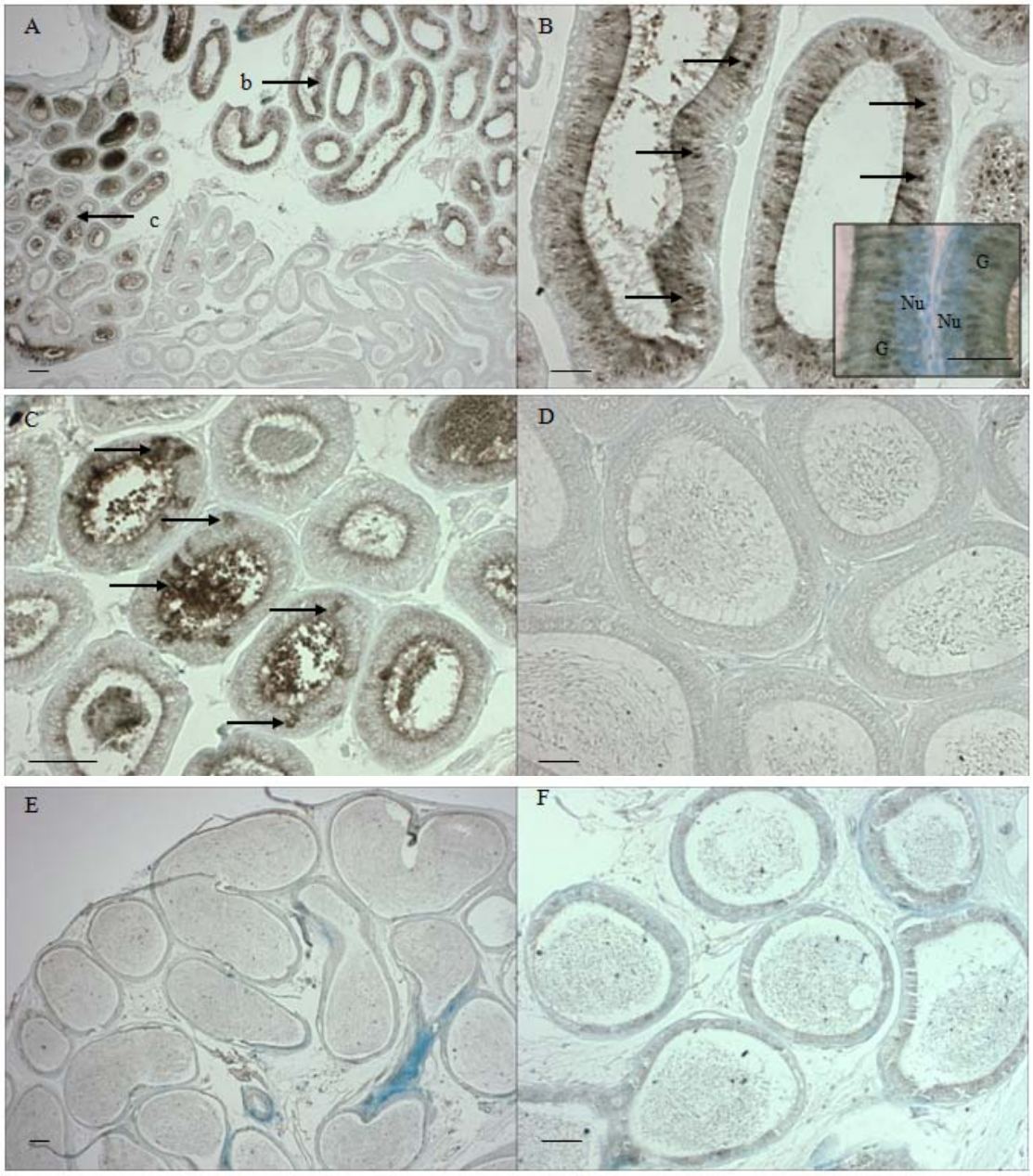
A
b
c
B
G
Nu
Nu
G
C
D
E
F

Further distally in the epididymis from this area of intense staining in the initial segment epithelium, the principal cells of the proximal caput were unreactive for CRES (Figure 16 C). This suggests that while CRES secretion has stopped, luminal CRES remains present as it flows downstream from the initial segment. However the clear cells were intensely stained, indicative of absorption of luminal CRES (Figure 16 C).

By mid-caput and distally along the epididymis no CRES immunostaining was evident in the epididymal epithelium (Figure 16 D, E, F). However, sperm tails throughout the epididymis, when cut transversally, were immunoreactive for CRES. In these cases, the epitopes in the ODF were most likely exposed by sectioning, whereas they would otherwise be inaccessible to antibodies. These results corroborate the present study's findings that CRES first produced in the testes associates with the ODF and remains through epididymal transit.

3.3.2 Western blot suggests CRES associates transiently with the sperm surface

Changes to the spermatozoon surface occur as it interacts with the luminal environment during epididymal transit, and the luminal environment is tightly regulated. While the CRES secretory activity of the principal cells in the initial segment in the epididymis has been demonstrated previously and confirmed in this study, it remains uncertain whether or not CRES merely remains in the epididymal lumen, or associates with the surface of spermatozoa. Thus, we explored the possibility of the transient or permanent association of CRES with the plasmalemma of epididymal sperm.

A non-ionic detergent extraction of similar numbers of thoroughly washed spermatozoa isolated from the caput and cauda epididymis was performed, followed by

immunoblotting of the extracts with anti-CRES, to determine if CRES is found superficially on the sperm surface. Thorough washing ensured proteins bound non-specifically from spermatozoa were removed. This was necessary because CRES is present in the epididymal luminal environment, and the objective was to determine if CRES was bound to the sperm surface in a specific manner. Western blot results show two major anti-CRES-reactive proteins of 14- and 19 kDa and a minor 17 kDa protein extracted from caput but not from cauda sperm (Figure 17 A). These bands correspond to a 14 kDa CRES isoform which is N-glycosylated to a size of 19 kDa, and a 17 kDa N-glycosylated form of a 12 kDa CRES protein [66], suggesting that both glycosylated and non-glycosylated CRES is secreted by the initial segment epithelium, and that these isoforms become associated with the surface of spermatozoa. It is not known why the 12 kDa CRES protein does not appear in these extracts – it is possible that all of these proteins are N-glycosylated in the Golgi apparatus of principal cells to the 17 kDa form before secretion, in contrast with the 14 kDa CRES protein, not all of which appears to be glycosylated to the 19 kDa form before secretion. No reactive bands are found in the extract from cauda epididymal spermatozoa (Figure 17 A), and since no immunoperoxidase staining was found in this study to be present in the cauda epididymis, these data suggest that surface-associated CRES in the caput epididymis has been removed before the sperm reaches the cauda.

In spermatozoa from both the caput and cauda epididymis, a 14 kDa anti-CRES reactive band is found to be insoluble with non-ionic detergent extraction (Figure 17 A). This band corresponds to a 14 kDa anti-CRES reactive band found in isolated sperm tails and coincident with an immunogold label over the ODF.

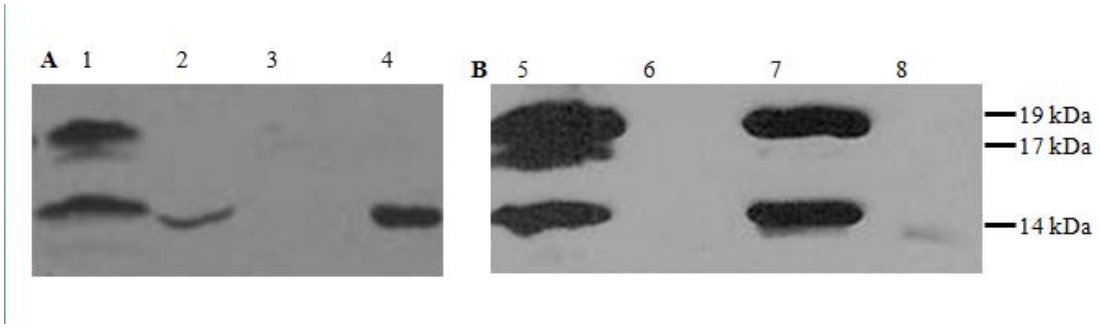

Figure 17

A Western blot of NP40 extracted cauda and caput sperm, as well as cauda and caput tissue and luminal fluid. Approximately 1 x 10^7 sperm were extracted and loaded onto a 13.5% SDS-PAGE gel, and in (A), (1) shows the NP40 extraction of caput sperm, (2) shows the pellet after NP40 extraction of caput sperm, (3) shows the NP40 extraction of cauda sperm, and (4) shows the pellet after NP40 extraction of cauda sperm. In (B), lanes (5)-(8), extracts of caput and cauda epididymal tissues and fluid were loaded as described in Chapter 2.5.1; (5) shows caput epididymal tissue, (6) shows cauda epididymal tissue, (7) shows caput epididymal luminal fluid, and (8) shows cauda epididymal luminal fluid.

The presence of 14- and 19- kDa anti-CRES reactive bands extracted with non-ionic detergent in caput, but not cauda spermatozoa, is coincident with data showing these two isoforms being present in isolated caput tissue and luminal fluid but not in cauda tissue or luminal fluid (Figure 17 B). In both caput epididymal tissue and luminal fluid, 14- and 19 kDa anti-CRES reactive bands are found, which correspond to previously reported glycosylated and non-glycosylated CRES isoforms, further suggesting that both of these isoforms are secreted by the principal cells of the initial segment. Since no reactive bands are found in cauda epididymal tissue or fluid, this corroborates data previously published and confirmed in this study that CRES is not secreted by the cauda epididymis.

These data are confirmed by immunoblotting analysis of physically fractionated samples of spermatozoa, in which all sperm fractions are accounted for. The sonicated supernatant contains the acrosomal contents, plasma membrane, and outer acrosomal membrane. The isolated sonicated sperm heads fraction contain the nucleus, perinuclear theca, and inner acrosomal membrane, while the isolated sonicated sperm tails fraction contain the axoneme, outer dense fibres, fibrous sheath, and mitochondrial sheath. In this manner, we are able to separate the functional components of spermatozoa in a way that detergent extractions could not. These data complement the present study's findings regarding NP40 extracted caput and cauda epididymal spermatozoa. The NP40 soluble fraction contains everything within the sonicated supernatant fraction, but also includes the inner acrosomal membrane, while the NP40 insoluble fraction contain everything else in isolated sonicated sperm heads and tails.

Western blots reveal that CRES resides exclusively to the tails in cauda spermatozoa, where a 14 kDa anti-CRES reactive band is visible in the isolated tail fraction (Figure 18). No anti-CRES reactive bands are detected in the isolated heads or sonicated supernatant fractions of cauda spermatozoa (Figure 18). This effectively rules out acrosomal localization of CRES in cauda epididymal spermatozoa.

However, in caput spermatozoa, a different picture arises. Three anti-CRES reactive bands were detected in the soluble fraction after sonication of caput spermatozoa of size 14-, 17-, and 19 kDa which correspond to glycosylated and non-glycosylated CRES isoforms (Figure 18). Trace amounts of a 14 kDa anti-CRES reactive band is found in isolated heads, and only a major 14 kDa band is found in isolated tails (Figure 18).

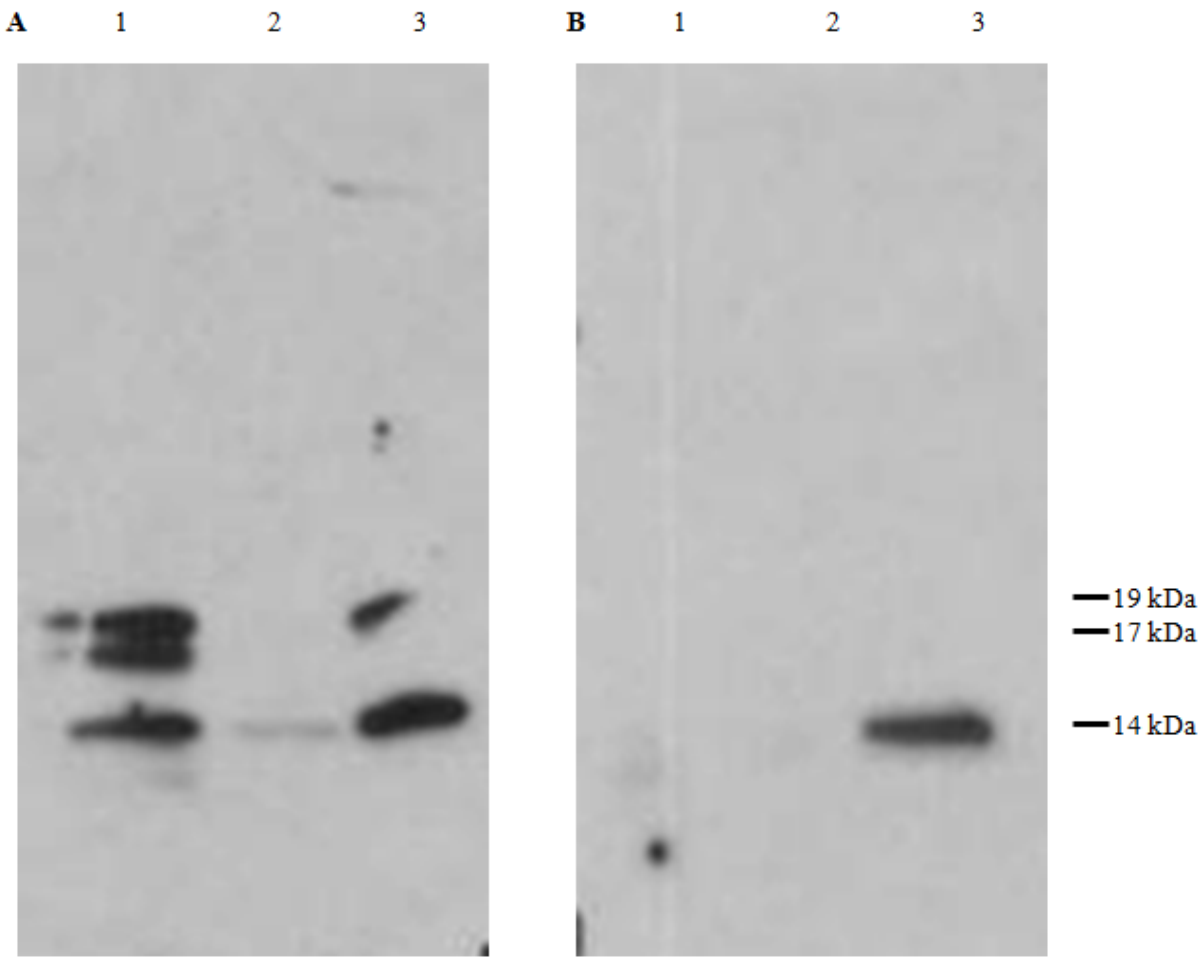

Figure 18

Western blot analysis of (A) caput and (B) cauda epididymal spermatozoa separated into different fractions, where (1) shows the sonicated supernatant, (2) shows isolated sonicated sperm heads, and (3) shows isolated sonicated sperm tails. The contents of approximately 1 x 10^7 spermatozoa were loaded in each lane.

Chapter 4 – Discussion

4.1 Where CRES Localizes and Originates

Localization is a very important step in determining the function of any protein found in spermatozoa. Since different compartments of spermatozoa perform different functions, the localization of a protein in a specific compartment or compartments will aid greatly in determining its functional significance. This study shows that there are two origins and areas of localization of CRES, which is summarized in Figure 19.

4.1.1 CRES associating with the ODF originates in the testis

Cauda spermatozoa, ready for ejaculation, contain only one isoform (14 kDa) of CRES, located within the ODF of the sperm tail. It is synthesized and assembled in the testis during spermatid elongation and maturation in spermiogenesis. The present study also finds CRES present in the connecting piece, which is not unexpected, as the ODF and connecting piece striated columns are continuous, and other ODF proteins have also been shown to be found in the connecting piece [1, 81]. This is the first time that CRES has been shown to be associated with both the ODF of the sperm tail and possibly the surface of sperm in the caput epididymis. From a developmental point of view this is not a surprise as CRES shows the same pattern of expression as ODF proteins [11, 81], with the expression starting in late round spermatids and ending at the end of the maturation phase of spermiogenesis (Figure 20).

4.1.2 CRES transiently associates with the sperm surface in the epididymis

However, during transit through the caput epididymis, the data in this study suggest maturing spermatozoa acquire two other CRES isoforms (17- and 19 kDa) on

Figure 19

Diagrammatic representation showing changes in CRES localization throughout epididymal transit. The red and yellow X and O symbols represent CRES isoforms and are explained in the table at the bottom of the figure. The spermatozoon is blue and the epididymal epithelium is green. Spermatozoa at spermiation contain only non-glycosylated CRES which is found in the outer dense fibres, and this originates from the testis in spermatogenesis. Upon entering the initial segment of the epididymis, they obtain glycosylated and non-glycosylated CRES on their surface which originates from secretions of the epididymal epithelium. Further distally in the caput epididymis, luminal as well as sperm surface associated CRES is removed and endocytosed by the clear cells of the epididymal epithelium. When the sperm reaches the cauda epididymis, only the initial CRES population found in the outer dense fibres remain. Note that no glycosylated CRES originating from the testis is found on spermiated spermatozoa.

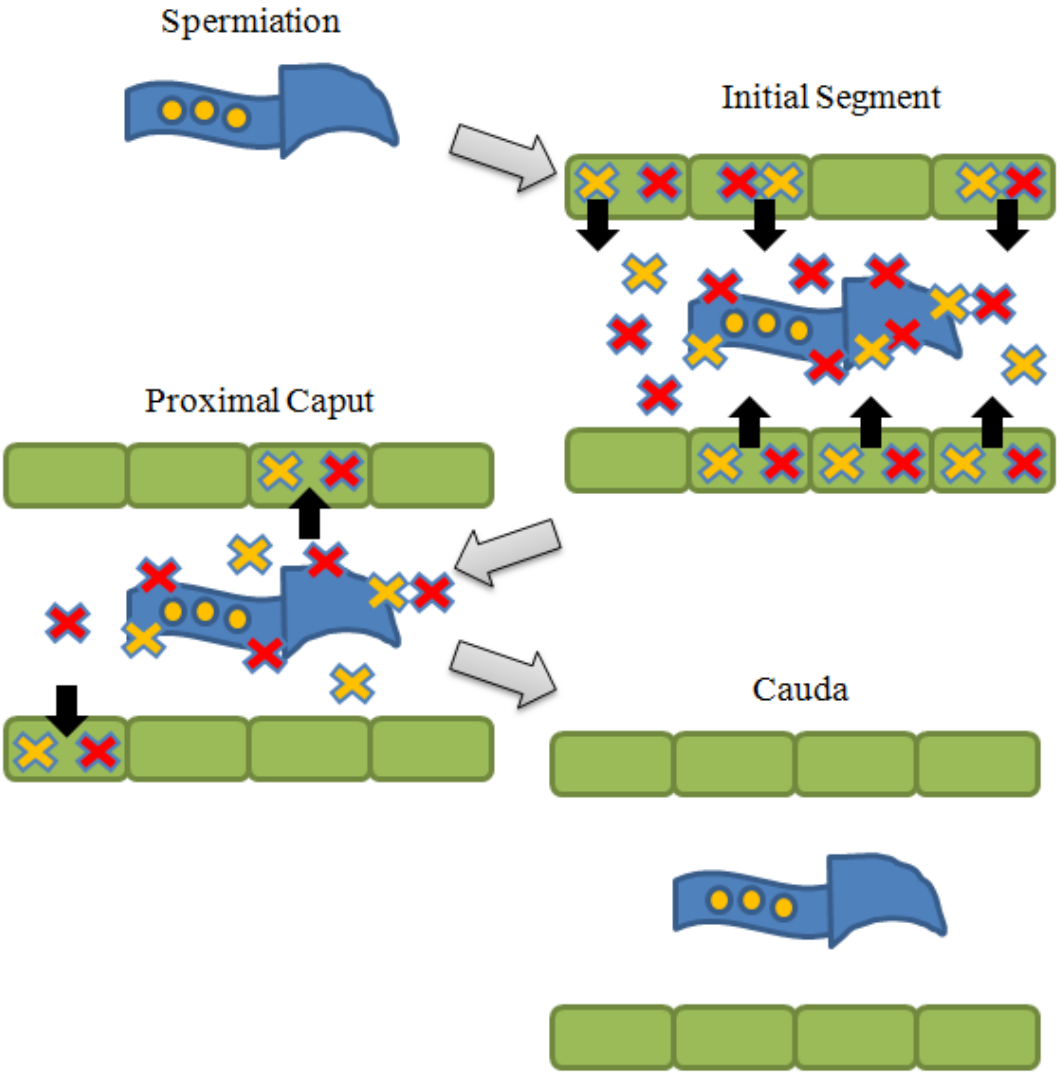

Origin	Glycosylated	Non-glycosylated
Testis	●	○
Epididymis	✕	✕

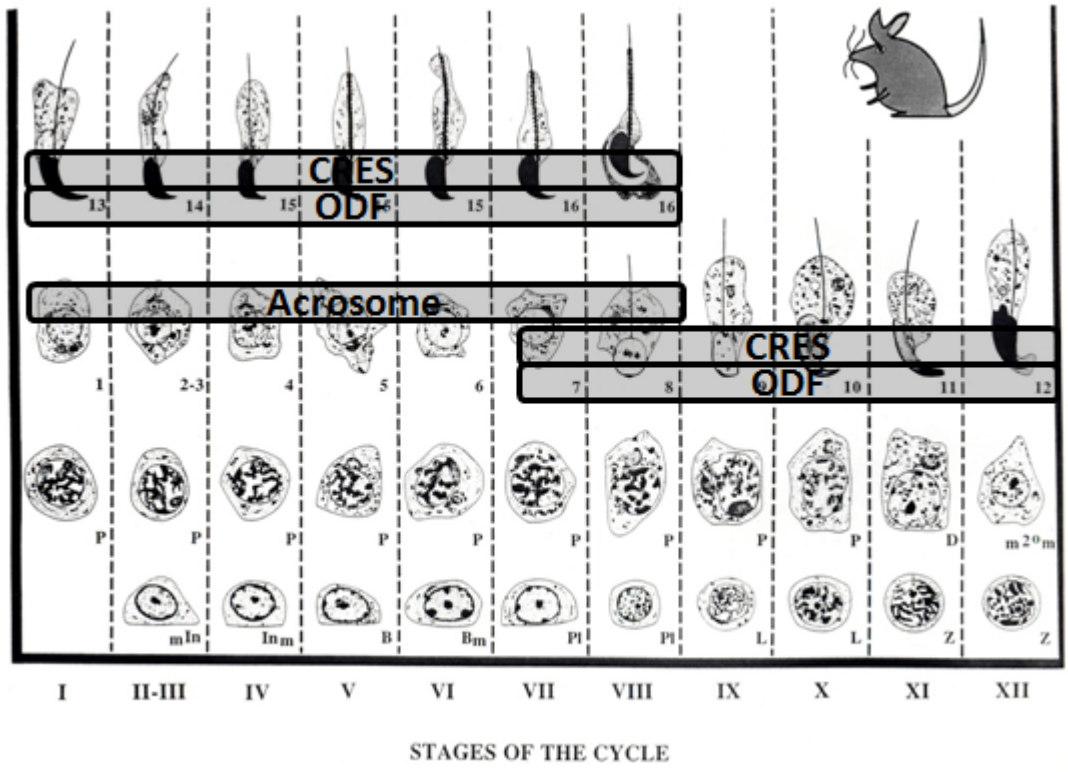

Figure 20

Diagrammatic representation showing the stages of the cycle of the seminiferous epithelium, and overlapping levels of CRES and ODF testicular expression, as well as stages in which the acrosome forms. Adapted from Russell et al. (1990) [15].

their surface which likely originate from secretions of the principal cells in the caput epithelium, which disappear by the time the sperm reaches the cauda epididymis. It is the presence of both glycosylated and non-glycosylated CRES in the NP40 soluble and sonicated supernatant fraction of caput, but not of cauda, spermatozoa in the epididymis, as well as the presence of glycosylated and non-glycosylated CRES in caput epididymal tissues and luminal fluids, which suggests that it is present superficially on the sperm surface of caput spermatozoa. If CRES were present either on the sperm surface or the acrosome in the cauda, then it should be present in the NP40 soluble fraction and in the sonicated supernatant; however, this is not the case.

The very low levels of what is presumably 14 kDa non-glycosylated CRES found in isolated heads in caput spermatozoa may come from a small amount of sperm tail contamination. It is possible that since the spermatozoon tail contains much more protein than the head, CRES found in a small number of contaminating residual tails found in the isolated heads sample might cause reactivity with anti-CRES. Indeed, the isolated tails of caput spermatozoa possess much higher levels of this 14 kDa anti-CRES reactive band.

Glycosylation of 12- and 14 kDa CRES isoforms to 17- and 19 kDa, respectively, was demonstrated by Sutton, Fusco, and Cornwall, by incubating epididymal and testicular tissue lysates in N-glycosidase F and examining them by immunblotting [66]. After treatment, 12- and 14 kDa immunoreactive bands increased in intensity, while 17- and 19 kDa bands disappeared, indicating that the 12- and 14- kDa CRES isoforms were N-link glycosylated. The presence of both glycosylated and non-glycosylated CRES isoforms in both caput epididymal tissues and luminal fluid suggest that two active methods of CRES secretion may be present: glycosylated CRES may be packaged and

secreted via vesicles by the Golgi apparatus, and non-glycosylated CRES may be secreted without Golgi modification via epididymosomes. Epididymosomes are blebs of cytoplasmic material which pinch off from principal cells of the epididymal epithelium and enter the lumen, and are involved in the delivery of new sperm proteins during epididymal transit [40, 82]. The disappearance of CRES from the NP40 soluble fraction of spermatozoa as it travels from the caput into the cauda epididymis suggests that it disappears from the sperm surface.

One possible mechanism of removal is disassociation of CRES from the sperm surface, followed by reabsorption and degradation by cells of the epididymal epithelium. It is possible that this occurs in the proximal caput epididymis, where clear cells in the epididymal epithelium are intensely stained, which indicates endocytosis of CRES from the epididymal lumen and, presumably, also the sperm surface. It is unlikely that this occurs further distally in the epididymis as we were unable to find further CRES expression in the epididymal epithelium. However, we cannot rule out a second possibility that surface CRES can be degraded on the sperm surface itself, or a third possibility that it may be removed from the sperm surface and degraded in the epididymal lumen, and that this occurs distally from the proximal caput epididymis. It is clear, however, that this occurs before the sperm reaches the cauda epididymis.

4.2 Where CRES Likely Does Not Localize

While this study provides extensive evidence that CRES associates with the ODF and transiently with the surface of spermatozoa, it also found no evidence that CRES can be found in other structures in mature spermatozoa, including in the acrosome, where it has been previously reported to be localized [72]. A major difference between the

present and past study lies in the use of different immune sera. While the present study used affinity purified anti-CRES antibody, Syntin and Cornwall did not affinity purify the immune serum used for immunogold electron microscopy and indirect immunofluoresence [72]. While absence of evidence is not evidence of absence, the present investigation concludes that CRES is likely not located in the following structures, for the following reasons.

4.2.1 The Acrosome

A previous report by Syntin and Cornwall localized CRES by immunofluorescence, immunocytochemistry, and immunoblotting to the acrosome of sperm [72] but this localization appears to be incompatible with other previously published data. First, acrosomal localization is incompatible with a lack of immunoreactivity in Western blotting analysis of Triton X-100 or SDS extractions of spermatozoa, which was performed in the same study by Syntin and Cornwall [72]. Secondly, acrosomal localization is very unlikely without a demonstration that CRES expression is present in round spermatids, where acrosomal formation occurs; both this study and Cornwall and Hann found testicular expression occurring mainly in elongating spermatids [69]. Those two findings are incompatible with results of immunogold electron microscopy and immunofluoresence studies that CRES is found in the acrosome [72]. Meanwhile, the present study is the first one performed where the results of Western blotting analysis of detergent extractions, immunoperoxidase staining of the testis and analysis of the cycle of the seminiferous epithelium, immunogold electron microscopy, and physical fractionation of spermatozoa all agree with each other.

This study confirms results of a previous study showing that CRES expression begins in late round spermatids and peaks in elongating spermatids [69]. In elongating spermatids, only morphological and physical changes occur to the acrosome, such as conforming to the change in shape of the nucleus as it elongates. While some acrosomal proteins undergo modifications or changes in intra-acrosomal localization during epididymal transit or post-translational changes in late spermiogenesis, testicular expression must begin and peak in round spermatids, and there is no precedent for acrosomal addition of proteins or mRNA after the round spermatid stage [56, 83, 84]. While the cytoplasm of elongating spermatids are intensely stained by the immunoperoxidase reaction, the spermatid heads are visibly free of labelling, and seen as clearly bright blue in Figure 7. The lack of labelling in the spermatid heads indicates that CRES does not reside in the acrosome.

The CRES mRNA has also been previously reported to be present only in round spermatids and elongating spermatids in stages VII-X [69]. It is not surprising that no further increase in CRES mRNA is observed after elongation begins [69], as nuclear chromatin condensation precludes further DNA transcription. Proteins required for latter phases of spermatogenesis must then be translated from mRNA produced in earlier stages which are stored. For several reasons, this translational delay is not a sufficient explanation as to how CRES might be localized in the acrosome. First, CRES mRNA disappears after stage X, and does not appear to be stored [69]. Second, there is no evidence that mRNA is packaged into the acrosome. Third, there is no evidence of ribosomes present in the acrosome. Fourth, by the time elongation begins in spermiogenesis, not only has transcription stopped, but the Golgi apparatus, which

delivered the contents of the acrosome in early spermiogenesis, has stopped performing this role as it is displaced caudally with much of the rest of the spermatid cytoplasm. Thus without the presence of CRES mRNA in the Golgi phase, gene expression beginning late in the cap phase, and only low levels of protein beginning to be detected late in the cap phase with the peak of protein expression occurring in the elongation phase (Figure 7), it does not appear that CRES is packaged by the Golgi apparatus for delivery into the acrosome.

It is noteworthy, however, that previously published data which was confirmed in this study shows an increase in CRES protein levels in elongating spermatids until stage XII, as indicated by the increasing intensity of the immunoperoxidase stain from stage VIII to XII. This data conflicts with previously published studies that show CRES mRNA disappears from elongating spermatids at stage X. If this were the case, then there is no source of mRNA for translation in stages XI and XII that would account for an increase in CRES protein levels in spermatids. A second look at the pattern of CRES expression in spermatids might be warranted. However, the presence of CRES mRNA in elongating spermatids after stage XII would be immaterial to the conclusions of this study, as no evidence exists that mRNA or ribosomes are present in acrosomes.

Furthermore, the NP40 soluble fraction contains the contents of the cellular membranes as well as the acrosome. While we found glycosylated and non-glycosylated CRES in the NP40 extract of caput spermatozoa, no CRES was found in the extract of cauda spermatozoa (Figure 17). We also found no detectable levels of CRES in the sonicated supernatant fraction of physically fractionated cauda spermatozoa, which contains most of the acrosomal contents, except the inner acrosomal membrane.

There is also no evidence found in this study of CRES presence in the acrosome after physical fractionation of spermatozoa. The soluble fraction after sonication of caput spermatozoa contains anti-CRES reactive bands (14-, 17-, and 19 kDa) corresponding to expected sizes of glycosylated and non-glycosylated CRES. However, these bands are not present in the sonicated supernatant of cauda spermatozoa. While an acrosomal matrix remains on the sperm head on the inner acrosomal membrane after induction of the acrosome reaction and release of acrosomal contents [76], CRES still cannot be present here. Should CRES be present in the inner acrosomal membrane coat, then it should be present in isolated sonicated sperm heads, where it would remain after sonication and release of acrosomal contents, concurrent with presence the NP40 soluble fraction, which would also solubilise the inner acrosomal membrane. Aside from the aforementioned lack of CRES expression in round spermatids, no anti-CRES reactive bands are found by immunoblotting in either the isolated heads of cauda spermatozoa or NP40 extract. This precludes the possibility that CRES present throughout the acrosome in the caput might undergo inter-acrosomal changes in localization to the inner acrosomal membrane coat in the cauda. This effectively rules out the possibility of CRES presence in the acrosome both in caput and cauda spermatozoa.

Lastly, no immunogold labelling was seen in the acrosome in this study when heads of spermatozoa were examined ultrastructurally in either testicular or cauda epididymal spermatozoa.

4.2.2 Other Structures in the Head

Based on this study's findings, no CRES is likely to be found in the nucleus or the perinuclear theca. This study initially considered localization to the perinuclear theca as

its formation is a defining event during the latter half of spermiogenesis [20]. Ultrastructural analysis revealed no immunogold labelling over the nucleus of spermatozoa incubated with anti-CRES followed by gold-conjugated secondary antibody in either the testicular or cauda epididymal spermatozoa. Furthermore, no anti-CRES reactive bands were visible in the isolated heads fraction of both caput and cauda spermatozoa when examined by immunoblotting (Figure 18), and this fraction contains both the nucleus and perinuclear theca.

4.2.4 Other Structures in the Tail

While some immunogold labelling can be seen in the mitochondrial sheath, the results of this study have determined that this labelling corresponds to a 66 kDa anti-CRES reactive protein visualized by immunoblotting which persists in *Cres* -/- mice. Using biochemical fractionation methods, we removed the MS from isolated tails of spermatozoa and found by immunoblotting that the 66 kDa reactive band was found in the extract, while a 14 kDa reactive band corresponding to the size of a non-glycosylated CRES isoform remained present in the pellet. We confirmed the localization of these bands by performing an ultrastructural analysis of extracted isolated tails, and determined that the 14 kDa protein resides in the ODF. Thus, the 66 kDa band is unrelated to CRES and is found in the ODF. There is no evidence of CRES in the MS as no anti-CRES reactive bands correspond to expected sizes of CRES isoforms which are not present in *Cres* -/- mice.

Furthermore, little to no immunogold label is found concentrated over the FS when we performed ultrastructural analyses of the tail.

4.3 Potential Roles of CRES in Reproduction

Previously published reports of CRES localization in human spermatozoa reveal striking differences between humans and mice. CRES has been reported to be localized to the equatorial segment in human spermatozoa with only very low levels of CRES mRNA expression in the epididymis [85], which is in stark contrast to the findings of this study in mice. It is certainly possible that CRES' role differs between humans and mice. However, a compounding factor between human and mouse comparisons include the age and health of subjects from which tissues and spermatozoa were obtained; human samples were provided by the Brain and Tissue Bank for Developmental Disorders at the University of Maryland [85], while the mice used in this study were retired breeders. Nonetheless, given that this study reached different conclusions than the previous CRES localization study performed in mice, it may be prudent that a second look should be given at human CRES localization as well. As such, it remains possible that CRES plays similar roles in mice and humans. The following discussion of possible CRES functions, then, will focus on the results of this study.

4.3.1 Epididymal Maturation

The results of this study suggest that CRES may play an important role in epididymal maturation. The process of epididymal maturation involves removal and addition of proteins on the sperm surface. Glycoprotein modifying enzymes are secreted by the epididymal epithelium and have been shown to cause modifications on the sperm surface [52]. The presence of glycosylated and non-glycosylated CRES isoforms in the luminal environment coincident with a likely appearance of CRES superficially on the sperm surface strongly suggests that luminal CRES is the source of any superficial CRES

association with spermatozoa. It is possible that some CRES found in epididymal luminal fluid may have come from principal cells of the epididymal epithelium which were broken during sperm collection. However, the presence of CRES in the epididymal luminal environment has also been shown in previously published data [69]. The strong immunoperoxidase stain of the Golgi apparatus of principal cells of the epididymis also strongly suggests that CRES is secreted by these cells into the lumen. Furthermore, the levels of CRES found in the luminal fluid is comparable to that found in tissues (Figure 17), and it is unlikely that that many cells were lysed during the sperm collection method. Thus, much of the CRES protein detected in the luminal environment by immunoblotting is likely due to active secretion into the lumen. The role that CRES plays in this process should be further examined to determine its role in reproduction.

Epididymal expression of CRES in the epididymal epithelium appears to be very tightly regulated. One reason is to properly regulate epididymal maturation. The mechanisms which cause changes to spermatozoa during epididymal transit must be highly regulated to succeed and properly create the region-specific microenvironments required for proper maturation [86]. Protease inhibitors may play an important role in ensuring proper protein processing of the high level of proteins and proteases which are found in the epididymal milieu. While the specific targets of CRES *in vivo* remain enigmatic, a first possibility is that this target for inhibition is similarly tightly regulated, and only persists in the initial segment of the caput epididymis. Thus CRES is not needed further distally in the epididymis. However, cells appear to actively remove CRES from the epididymal lumen, and the likely CRES presence on the surface of spermatozoa is similarly removed or degraded. Thus active removal or degradation of

CRES opens a second possibility that its inhibitory target might need to be turned on further distally in the epididymis. Active CRES removal might also suggest that CRES may cause improper maturation if present distally in the epididymis or another kind of physiological harm.

So a third possibility for tight regulation of CRES expression may be to prevent toxicity and pathology. CRES has also been shown to have the ability to form oligomeric amyloid fibres, which could cause toxicity and pathology in the epididymis if not removed [87]. For example, amyloid aggregations have been shown to be associated with pathologies in the brain and are implicated in Alzheimer's disease [88]. While no amyloid diseases have yet to be described for the epididymis, this may be a testament to the effectiveness epididymal quality control mechanisms. Thus, CRES removal from the epididymal lumen might not be required simply for the regulation of epididymal maturation, but also to protect against toxicity.

On the other hand, CRES associated with the ODF is not removed or degraded during epididymal transit. It is likely inaccessible to the mechanisms in the epididymal lumen which modify surface CRES, and this is likely why CRES found in the sperm tail is not removed or degraded during epididymal transit. Furthermore, its sequestration in the sperm tail separates it from the epididymal lumen and from oligomerization with secreted epididymal CRES. As such, its presence would be unlikely to cause pathologies associated with amyloidogenesis and improper oligomerization.

4.3.2 Motility and Capacitation

The ODF are composed mainly of Odf1, Odf2, as well as accessory proteins, and interact with each other mainly via leucine zippers [81, 89]. The numerous accessory proteins of the sperm tail have been implicated to play a role in structural function, glycolysis, cell signalling, and metabolism [6]. The presence of CRES in the ODF, and its pattern of expression in the testis in development, suggests that it may play a role in regulating enzymatic processes important for tail formation, mediating protein-protein interactions, and sperm motility.

Serine protease inhibitors have been shown to be able to both inhibit motility as well as prevent its initiation [90] and regulation of their activity with inhibitors may be important for proper maturation. Since CRES is a serine protease inhibitor, its localization to the ODF suggests it may play a role in regulating motility.

Furthermore, one of the hallmark changes in spermatozoa after capacitation is hyper-motility. *Cres* -/- mice also exhibit decreased tyrosine phosphorylation associated with capacitation (unpublished data from Dr. Gail Cornwall, Department of Cell Biology and Biochemistry, Texas Tech University Health Sciences Centre, Lubbock, Texas). Sperm motility is initiated and maintained by cyclic adenosine monophosphate (cAMP) dependent phosphorylation of tail proteins, and protein kinase A (PKA), which is a major downstream target of cAMP, has been implicated as a key step in this pathway [91, 92, 93]. Furthermore, spermatozoa acquire the potential to exhibit cAMP dependent tyrosine phosphorylation of the tail during epididymal maturation in the caput epididymis [94], where CRES is present in both the luminal environment and on the sperm surface. It is then warranted in future studies examine not only the structure of ODF and its

relationship to the axoneme in spermatozoa from *Cres* -/- mice, but also to examine differences in sperm motility using computer assisted sperm analysis.

Since capacitation is mainly an interaction between the surface of spermatozoa and the environment of the female reproductive tract, the signal transduction pathway which signals phosphorylation of tail proteins is thus important to deliver signals which trigger hyper-motility associated with capacitation. While we have shown that CRES on the sperm surface is removed during epididymal transit, this suggests that its effects on its targets, potentially involved in this signal transduction pathway, could persist. Alternatively, it might regulate downstream targets of this pathway in the sperm tail itself, where it is present after epididymal maturation and presumably after ejaculation.

Indeed, it has recently been shown that spermatozoa from *Cres* -/- mice exhibit a reduced ability to bind the zona pellucida and fuse with the oolemma (Cornwall, G A, unpublished data). It is possible that it regulates other important components of the sperm surface which persist on spermatozoa after CRES has been removed, and mediate zona pellucida binding and oolemma fusion. Actions of PKA on target downstream kinases, and the activity of these kinases, may require regulation by enzymatic inhibitors to ensure proper function. As CRES is present in the tail of ejaculated spermatozoa, it may regulate important proteins downstream of PKA in this signal transduction pathway, and as such, these downstream targets of PKA should be examined as potential *in vivo* targets of CRES inhibitory activity.

4.4 Future Directions

4.4.1 Visualization of Surface-Associated CRES

While the results of this study's immunoblotting analysis of sperm fractions by biochemical and physical separation strongly suggest that CRES found in the non-ionic detergent soluble fraction and in the sonicated supernatant originate from epididymal secretions and reside on the sperm surface, visualization of this localization would create a more definitive conclusion. There are two ways to accomplish this: pre-embedding immunogold labelling and indirect immunofluoresence.

The fixation and processing procedure for post-embedding immunogold labelling used in this study and that of Syntin and Cornwall [72] involved the use of harsh solutions including glutaraldehyde, ethanol, and LR white. Exposure to these chemicals may remove, degrade, modify, or otherwise make it possible that antigens present on the surface of spermatozoa are made inaccessible to the anti-CRES antibody for immunolabelling. Altering the procedure to expose spermatozoa to anti-CRES while in suspension in PBS *before* fixation and embedding will allow the anti-CRES antibody to bind to surface antigens before they are exposed to harsh conditions. Based on the results of this study, it can be hypothesized that performing pre-embedding labelling with spermatozoa from the initial segment and proximal caput epididymis might reveal the presence of CRES on the sperm surface, while there should be no surface labelling in cauda spermatozoa.

Post-fixation indirect immunofluoresence was used by the study conducted by Syntin and Cornwall which concluded CRES was localized to the acrosome of

spermatozoa [72]. That study found that the fluorescent signal representing CRES protein in non-permeabilized spermatozoa (where only surface-associated antigens are exposed) is no different from a background signal, while the fluorescent signal in permeabilized spermatozoa (where surface-associated and acrosomal antigens are exposed) showed a signal over the acrosomal region. The fixation and processing procedure in the immunofluoresence protocol might alter surface-associated antigens in a similar manner as previously discussed with post-embedding immunogold labelling. Pre-fixation labelling followed by indirect immunofluoresence thus might reveal the presence of CRES on the surface of spermatozoa.

4.4.2 Sperm Motility Analysis

The results of this study point to a potential role that CRES might play in regulating sperm motility. A comparison of motility patterns of spermatozoa from *Cres* -/- and wild-type mice using computer-aided sperm analysis might reveal these potential changes. Different sperm motility patterns have been associated with enhanced fertilizing capability in both mouse and human spermatozoa [95, 96]. Thus, any fertilization deficiency from spermatozoa from *Cres* -/- mice might be due to a problem with motility, and this possibility should be examined.

4.4.3 Development and Maturation

Given the stage-specific expression of CRES in spermatogenesis, it is possible that it plays an important role in the formation of the sperm tail. Abberations in normal spermatogenesis might be seen in spermatozoa from *Cres* -/- mice, and the ultrastructure of these spermatozoa should be examined. Elongating spermatids from *Cres* -/- mice appear to possess tails suspended in the lumen of the seminiferous tubule (Figure 6 B).

However, it has been shown that underlying structural defects might be present in spermatozoa which otherwise appear morphologically normal when examined under light microscopy [97].

Previous studies detailing the expression of CRES mRNA have shown that no more CRES mRNA is expressed after step 10 (stage X) elongating spermatids [69]. This cannot explain the increase in CRES protein levels until step 12 (stage XII) elongating spermatids seen in previous studies and confirmed in the present one; if no CRES mRNA exists in step 11 and step 12 spermatids, then there should be no mRNA available for translation and protein synthesis. A second look at CRES mRNA expression in the seminiferous epithelium is thus warranted, with an examination to see if the mRNA is sequestered in some way that is inaccessible to *in situ* hybridization experiments.

4.4.4 CRES *In Vivo* Target

CRES has been shown to target PC2 in *in vitro* studies [68]. A demonstration that PC2 is present either in mammalian spermatozoa or in the epididymal epithelium and/or secretions followed by an *in vivo* demonstration of CRES inhibitory action on PC2 is thus the next necessary step in determining if CRES inhibition of PC2 is physiologically relevant.

4.5 Summary

The main contribution of this study to the field of reproductive biology is the finding that CRES is a component of the outer dense fibres. Another important contribution is the strong suggestion that CRES secreted from the principal cells of the epididymal epithelium likely transiently associates with the surface of caput epididymal

spermatozoa, and that surface-associated CRES appears to be removed and endocytosed by the clear cells of the epididymal epithelium. Fully mature cauda epididymal spermatozoa contain only CRES which is a component of the ODF. These data point to a possible important role that CRES might play in fertility and sperm motility which needs further investigation.

References

1. Fawcett, D. W. (1975). The mammalian spermatozoon. *Dev Biol* , 44: 394-436.

2. Escalier, D. (2003). New Insights into the Assembly of the Periaxonemal Structures in Mammalian Spermatozoa. *Biol Reprod* , 69(2): 373-378.

3. Tash, J. S., & Means, A. R. (1982). Regulation of protein phosphorylation and motility of sperm by cyclic adenosine monophosphate and calcium. *Biol Reprod* , 26(4): 745-763.

4. Gibbons, I. R., & Rowe, A. J. (1965). Dynein: a protein with ATPase activity from cilia. *Science* , 149: 424-426.

5. Ostrowski, L. E., Blackburn, K., Radde, K. M., Moyer, M. B., Schlatzer, D. M., Moseley, A., et al. (2002). A proteomic analysis of human cilia: identification of novel compoenents. *Mol Cell Proteomics* , 1: 451-465.

6. Cao, W., Gerton, G. L., & Moss, S. B. (2006). Proteomic Profiling of Accessory Structures from the Mouse Sperm Flagellum. *Mol Cell Proteomics* , 5: 801-810.

7. Sutovsky, P., Tengowski, M. W., Navara, C. S., Zoran, S. S., & Schatten, G. (1997). Mitochondrial sheath movement and detachment in mammalian, but not nonmammalian, sperm induced by disulfide bond reduction. *Mol Reprod Dev* , 47: 79-86.

8. Miki, K., Qu, W., Goulding, E. H., Willis, W. D., Bunch, D. O., Strader, L. F., et al. (2004). Glyceraldehyde 3-phosphate dehydrogenase-S, a sperm-specific glycolytic

enzyme, is required for sperm motility and male fertility. *PNAS* , 101(47): 16501-16506.

9. Mukai, C., & Okuno, M. (2004). Glycolysis plays a major role for adenosine triphosphate supplementation in mouse sperm flagellar movement. *Biol Reprod* , 71(2): 540-547.

10. Eddy, E. M., Toshimori, K., & Deborah, A. O. (2003). Fibrous Sheath of Mammalian Spermatozoa. *Micr Res Tech* , 61: 103-115.

11. Oko, R., & Clermont, Y. (1991). Biogenesis of specialized cytoskeletal elements of rat spermatozoa. *Ann N Y Acad Sci* , 637: 203-223.

12. Irons, M. J., & Clermont, Y. (1982). Kinetics of fibrous sheath formation in the rat spermatid. *Am J Anat* , 165: 121-130.

13. Irons, M. J., & Clermont, Y. (1982). Formation of the outer dense fibres during spermiogenesis in the rat. *Anat Rec* , 202(4): 463-471.

14. Dym, M., & Clermont, Y. (1970). Role of spermatonogia in the repair of the seminiferous epithelium following X-irradiation of the rat testis. *Am J Anat* , 128: 265-282.

15. Russell, L., Ettlin, R., Sinha Hikim, A., & Clegg, E. (1990). *Histological and Histopathological Evaluation of the Testis.* Clearwater: Cache River Press: St Louis, Missouri.

16. Cooper, T. G. (2005). Cytoplasmic droplets: the good, the bad or just confusing? *Hum Rep* , 20(1): 9-11.

17. Oko, R., Hermo, L., Chan, P. T., Fazel, A., & Bergeron, J. J. (1993). The cytoplasmic droplet of rat epididymal spermatozoa contains saccular elements with Golgi characteristics. *J Cell Biol* , 123(4): 809-821.

18. Olson, G. E., & Winfrey, V. (1991). Structure-function relationships and the sperm acrosome. *Ann N Y Acad Sci* , 637: 240-257.

19. Oko, R., & Maravei, D. (1995). Distribution and possible role of perinuclear theca proteins during bovine spermiogenesis. *Micr Res Tech* , 32: 520-532.

20. Oko, R., & Sutovsky, P. (2009). Biogenesis of sperm perinuclear theca and its role in sperm functional competence and fertilization. *J Reprod Immunol* , 83(1): 2-7.

21. Kimura, Y., Yanagimachi, R., Kuretake, S., Bortkiewicz, H., Perry, A. C., & Yanagimachi, H. (1998). Analysis of mouse oocyte activation suggests the involvement of sperm perinuclear material. *Bio Reprod* , 58(6): 1407-1415.

22. Wu, A. T., Sutovsky, P., Manandhar, G., Xu, W., Katayama, M., Day, B. N., et al. (2007). PAWP, a sperm-specific WW domain-binding protein, promotes meiotic resumption and pronuclear development during fertilization. *J Biol Chem* , 282: 12164-12175.

23. Aul, R. B., & Oko, R. (2002). The major subacrosomal occupant of bull spermatozoa is a novel histone H2B variant associated with the forming acrosome during spermiogenesis. *Dev Biol* , 242: 376-387.

24. Heid, H., Figge, U., Winter, S., Kuhn, C., Zimbelmann, R., & Franke, W. (2002). Novel actin-related proteins Arp-T1 and Arp-T2 as components of the cytoskeletal calyx of the mammalian sperm head. *Exp Cell Res* , 279: 177-187.

25. Rousseaux-Prevost, R., Lecuyer, C., Drobecq, H., Sergheraert, C., Dacheux, J. L., & Rousseaux, J. (2003). Characterization of boar sperm cytoskeletal cylicin II as an actin-binding protein. *Biochem Biophys Res Commun* , 303: 182-189.

26. McLachlan, R. I., Rajpert-De Meyts, E., Hoei-Hansen, C. E., de Krester, D. M., & Skakkebaek, N. E. (2007). Histological evaluation of the human testis - approaches to optimizing the clinical view of the assessment: Mini Review. *Human Reproduction* , 22(1): 2-16.

27. Fawcett, D. W., Neaves, W. B., & Flores, M. N. (1973). Comparative Observations on Intertubular Lymphatics and the Organization of the Interstitial Tissue of the Mammalian Testis. *Biol Reprod* , 9(5): 500-532.

28. Mori, H., & Christensen, A. K. (1980). Morphometric Analysis of Leydig Cells in the Normal Rat Testis. *J Cell Biol* , 84: 340-354.

29. Yan, H. H., Mruk, D. D., & Cheng, C. Y. (2008). Blood-testis barrier dynamics are regulated by testosterone and cytokines via their differential effects on the kinetics of protein endocytosis and recycling in Sertoli cells. *FASEBJ* , 22: 1945-1959.

30. Dube, E., Chan, P. T., Hermo, L., & Cyr, D. G. (2007). Gene Expression Profiling and Its Relevance to the Blood-Epididymal Barrier in the Human Epididymis. *Biol Reprod* , 76(6):1034-1044.

31. Leblond, C. P., & Clermont, Y. (1952). Definition of the stages of the cycle of the seminiferous epithelium in the rat. *Ann N Y Acad Sci* , 55(4): 548-573.

32. Leblond, C. P., & Clermont, Y. (1952). Spermiogenesis of rat, mouse, hamster, and guine pig as revealed by the periodic acid-fuchsin sulfurous acid technique. *Am J Anat* , 90(2): 167-215.

33. Oakberg, E. F. (1956). Duration of spermatogenesis in the mouse and timing of stages of the cycle of the seminiferous epithelium. *Am J Anat* , 99(3): 507-516.

34. Clermont, Y., & Leblond, C. P. (1953). Renewal of spermatogonia in the rat. *Am J Anat* , 93(3): 475-501.

35. Fawcett, D. W., Ito, S., & Slautterback, D. (1959). The occurence of intercellular bridges in groups of cells exhibiting synchronous differentiation. *J Biophys Biochem Cytol* , 5(3): 453-460.

36. Dym, M., & Fawcett, D. W. (1971). Further observations on the numbers of spermatogonia, spermatocytes, and spermatids connected by intercellular bridges in the mammalian testis. *Biol Reprod* , 4(2): 195-215.

37. Clermont, Y. (1972). Kinetics of Spermatogenesis in Mammals: Seminiferous Epithelium Cycle and Spermatogonial Renewal. *Physiol Rev* , 52 (1): 198-236.

38. Clermont, Y., Oko, R., & Hermo, L. (1993). Cell Biology of Mammalian Spermiogenesis. In C. Desjardins, & L. L. Ewing, *Cell and molecular biology of the testis* (pp. 332-375). Oxford Univ Press: New York City.

39. Robaire, B., & Viger, R. (1995). Regulation of Epididymal Epithelial Cell Functions. *Biol Reprod* , 52: 226-236.

40. Cornwall, G. A. (2009). New insights into epididymal biology and function. *Hum Reprod Update* , 15(2): 213-227.

41. Clulow, J., Jones, R. C., Hansen, L. A., & Man, S. Y. (1998). Fluid and electrolyte reabsorption in the ductuli efferentes testis. *J Reprod Fertil Suppl* , 53: 1-14.

42. Gadella, B. M., & van Gestel, R. A. (2004). Bicarbonate and its role in mammalian sperm function. *Anim Reprod Sci* , 307-319.

43. Kujala, M., Hihnala, S., Tienari, J., Kaunisto, K., Hastbacka, J., Holmberg, C., et al. (2007). Expression of ion transport-associated proteins in human efferent and epididymal ducts. *Reproduction* , 775-784.

44. Adamali, H., & Hermo, L. (1996). Apical and narrow cells are distinct cell types differing in their structure, distribution, and functions in the adult rat epididymis. *J Androl* , 17(3): 208-222.

45. Hermo, L., Dworkin, J., & Oko, R. (1988). Role of epithelial clear cells of the rat epididymis in the disposal of the conents of cytoplasmic droplets detached from spermatozoa. *Am J Anat* , 183(2): 107-124.

46. Vierula, M. E., Rankin, T. L., & Orgebin-Crist, M.-C. (1995). Electron microscopic immunolocalization of the 18 and 29 kilodalton secretory proteins in the mouse epididymis: Evidence for differential uptake by clear cells. *Micr Res Tech* , 30(1): 24-36.

47. Veri, J. P., Hermo, L., & Robaire, B. (1993). Immunocytochemical localization of the Yf subunit of glutathione S-transferase P shows regional variation in the staining of epithelial cells of the testis, efferent ducts, and epididymis of the male rat. *J Androl* , 14: 23-44.

48. Seiler, P., Cooper, T. G., & Nieschlag, E. (2000). Sperm number and condition affect the number of basal cells and their expression of macrophage antigen in the murine epididymis. *Int J Androl* , 23(2): 65-76.

49. Flickinger, C. J., Bush, L. A., Howards, S. S., & Herr, J. C. (1997). Distribution of Leukocytes in the Epithelium and Interstitium of Four Regions of the Lewis Rat Epididymis. *Anat Rec* , 248(3): 380-390.

50. Toshimori, K. (2003). Biology of Spermatozoa Maturation: An Overview With an Introduction to This Issue. *Micr Res Tech* , 61: 1-6.

51. Lakoski, K. A., Carron, C. P., Cabot, C. L., & Saling, P. M. (1988). Epiddiymal Maturation and the Acrosome Reaction in Mouse Sperm: Response to Zona Pellucida Develops Coincident with Modification of M42 Antigen. *Biol Reprod* , 38: 221-233.

52. Tulsiani, D., Orgebin-Crist, M., & Skudlarek, M. (1998). Role of luminal fluid glycosyltransferases and glycosidases in the modification of rat sperm plasma membrane glycoproteins during epididymal maturation. *J Reprod Fertil Suppl* , 52: 85-97.

53. Robarie, B., Hinton, B. T., & Orgebin-Crist, M.-C. (2006). The Epididymis. In J. D. Neill, *Knobil and Neill's Physiology of Reproduction (Third Edition)* (pp. 1071-1148). New York City: Elsevier.

54. Aitken, R. J., Nixon, B., Lin, M., Koppers, A. J., Lee, Y. H., & Baker, M. A. (2007). Proteomic changes in mammalian spermatozoa during epididymal maturation. *Asian J Androl* , 9(4): 554-564.

55. Cooper, T. G. (2007). Sperm maturation in the epididymis: a new look at an old problem. *Asian J Androl* , 9(4): 533-539.

56. Yoshinaga, K., Tanii, I., Saxena, D. K., & Toshimori, K. (1998). Immunocytochemical alterations in the intra-acrosomal antigen MN7 during epididymal maturation of guine pig spermatozoa. *Cell Tissue Res* , 292: 427-433.

57. Yoshinaga, K., & Toshimori, K. (2003). Organization and Modifications of Sperm Acrosomal Molecules During Spermatogenesis and Epididymal Maturation. *Micr Res Tech* , 61: 39-45.

58. Baker, M. M., Smith, N. D., Hetherington, L., Taubman, K., Graham, M. E., Robinson, P. J., et al. (2010). Label-Free Quantitation of Phosphopeptide Changes During Rat Sperm Capacitation. *J Proteome Res* , 9(2): 718-729.

59. Jones, R., James, P. S., Howes, L., Bruckbauer, A., & Klenerman, D. (2007). Supramolecular organization of the sperm plasma membrane during maturation and capacitation. *Asian J Androl* , 9: 438–444.

60. Fraser, L. R. (1984). Mouse sperm capacitation in vitro involves loss of a surface associated inhibitory component. *J Reprod Fertil* , 72: 373-384.

61. Nixon, B., MacIntyre, D. A., Mitchell, L. A., Gibbs, G. M., O'Bryan, M., & Aitken, R. J. (20006). The Identification of Mouse Sperm-Surface-Associated Proteins and Characterization of Their Ability to Act as Decapacitation Factors. *Biol Reprod* , 74(2): 275-287.

62. Gibbons, R., Adeoya-Osiguwa, S. A., & Fraser, L. R. (2005). A mouse sperm decapacitation factor receptor is phosphatidylethanolamine-binding protein 1. *Reproduction* , 130: 497-508.

63. Breitbart, H. (2002). Intracellular calcium regulation in sperm capacitation and acrosomal reaction. *Mol Cell Endocrinol* , 1(2): 139-144.

64. Oko, R., & Clermont, Y. (1989). Light microscopic immunocytochemical study of fibrous sheath and outer dense fiber formation in the rat spermatid. *Anat Rec* , 225(1): 46-55.

65. Cornwall, G. A., Orgebin-Crist, M., & Hann, S. (1992). The CRES gene: a unique testis-regulated gene related to the cystatin family is highly restricted in its expression to the proximal region of the mouse epididymis. *Mol Endocrinol* , 1653-1664.

66. Sutton, H. G., Fusco, A., & Cornwall, G. A. (1999). Cystatin-Related Epididymal Spermatogenic Protein Colocalizes with Luteinizing Hormone-ß Protein in Mouse Anterior Pituitary Gonadotropes. *Endocrinology* , 140 (6): 2721-2732.

67. Cornwall, G. A., Hsia, N., & Sutton, H. G. (1999). Structure, alternative splicing and chromosomal localization of the cystatin-related epididymal spermatogenic gene. *Biochem J* , 340: 85-93.

68. Cornwall, G. A., Cameron, A., Lindberg, I., Hardy, D. M., Cormier, N., & Hsia, N. (2003). The Cystatin-Related Epididymal Spermatogenic Protein Inhibits the Serine Protease Prohormone Convertase 2. *Endocrinology* , 144 (3): 901-908.

69. Cornwall, G. A., & Hann, S. R. (1995). Transient appearance of CRES protein during spermatogenesis and caput epididymal sperm maturation. *Mol Reprod Dev* , 41 (1): 37-46.

70. Yuan, Q., Guo, Q.-S., Cornwall, G. A., Xu, C., & Wang, Y.-F. (2007). Age-dependent expression of the cystatin-related epididymal spermatogenic (Cres) gene in mouse testis and epididymis. *Asian J Androl* , 9(3): 305-311.

71. Braun, R. E. (2000). Temporal control of protein synthesis during spermatogenesis. *Int J Androl* , 23(Suppl. 2): 92-94.

72. Syntin, P., & Cornwall, G. A. (1999). Immunolocalization of CRES (Cystatin-Related Epididymal Spermatogenic) Protein in the Acrosomes of Mouse Spermatozoa. *Biol Reprod* , 60 (6): 1542-1552.

73. Sutovsky, P., Manandhar, G., Wu, A., & Oko, R. (2003). Interactions of sperm perinuclear theca with the oocyte: Implications for oocyte activation, anti-polyspermy defense, and assisted reproduction. *Microsc Res Tech* , 61 (4): 362-378.

74. Yu, Y., Vanhorne, J., & Oko, R. (2009). The origin and assembly of a zona pellucida binding protein, IAM38, during spermiogenesis. *Micr Res Tech* , 72(8): 558-565.

75. Bleil, J. D., Greve, J. M., & Wassarman, P. M. (1988). Identification of a secondary sperm receptor in the mouse egg zona pellucida: Role in maintenance of binding of acrosome-reacted sperm to eggs. *Dev Biol* , 128(2): 376-385.

76. Yu, Y., Xu, W., Yi, Y.-J., Sutovsky, P., & Oko, R. (2006). The extracellular protein coat of the inner acrosomal membrane is involved in zona pellucida binding and penetration during fertilization: Characterization of its most prominent polypeptide (IAM38). *Dev Biol* , 290(1): 32-43.

77. Oko, R. (1988). Comparative analysis of proteins from the fibrous sheath and outer dense fibres of rat spermatozoa. *Biol Reprod* , 39: 169-182.

78. Olson, G. E., Hamilton, D. W., & Fawcett, D. W. (1976). Isolation and Characterization of the fibrous sheath of rat epididymal spermatozoa. *Biol Reprod* , 14(5): 517-530.

79. Laemmli, U. K. (1970). Cleavage of structural proteins during the assembly of the head of bacteriophage T4. *Nature* , 227(5259): 680-685.

80. Oko, R., Jando, V., Wagner, C., Kistler, W., & Hermo, L. (1996). Chromatin reorganization in rat spermatids during the disappearance of testis-specific histone, H1T, and the appearance of transition proteins TP1 and TP2. *Biol Reprod* , 54: 1141-1157.

81. Schalles, U., Shao, X., van der Hoorn, F. A., & Oko, R. (1998). Developmental Expression of the 84-kDa ODF Sperm Protein: Localization to both the Cortex and Medulla of Outer Dense Fibers and to the Connecting Piece. *Dev Biol* , 199(2): 250-260.

82. Sullivan, R., Frenette, G., & Girouard, J. (2007). Epididymosomes are involved in the acquisition of new sperm proteins during epididymal transit. *Asian J Androl* , 9(4): 483-491.

83. Toshimori, K. (1998). Maturation of mammalian spermatozoa: modifications of the acrosome and plasma membrane leading to fertilization. *Cell Tissue Res* , 293: 177-187.

84. Olson, G. E., Winfrey, V. P., & Nagdas, S. K. (2003). Structural modification of the hamster sperm acrosome during posttesticular development in the epididymis. *Micr Res Tech* , 61(1): 46-55.

85. Wassler, M., Syntin, P., Sutton-Walsh, H. G., Hsia, N., Hardy, D. M., & Cornwall, G. A. (2002). Identification and Characterization of Cystatin-Related Epididymal Spermatogenic Protein in Human Spermatozoa: Localization in the Equatorial Segment. *Biol Reprod* , 67(3): 795-803.

86. Turner, T. T., Bomgardner, D., Jacobs, J. P., & Nguyen, Q. A. (2003). Association of segmentation of the epididymal interstitium with segmented tubule function in rats and mice. *Reproduction* , 125: 871-878.

87. von Horsten, H., Johnson, S., SanFrancisco, S., Hastert, M. C., Whelly, S., & Cornwall, G. (2007). Oligomerization and Transglutaminase Cross-linking of the Cystatin CRES in the Mouse Epididymal Lumen. *J Biol Chem* , 282: 32912-32923.

88. Levy, E., Sastre, M., Kumar, A., Gallo, G., Piccardo, P., Ghetti, B., et al. (2001). Codeposition of Cystatin C with Amyloid-Beta Protein in the Brain of Alzheimer Disease Patients. *J Neuropathol Exp Neurol* , 60(1): 94-104.

89. Shao, X., Tarnasky, H. A., Lee, J., Oko, R., & van der Hoorn, F. A. (1999). Spag4, a Novel Sperm Protein, Binds Outer Dense Fibre Protein Odf1 and Localizes to Microtubules of Manchette and Axoneme. *Dev Biol* , 211(1): 109-123.

90. de Lamirande, E., & Gagnon, C. (1986). Effects of protease inhibitors and substrates on motility of mammalian spermatozoa. *J Cell Biol* , 102 (4): 1378-1383.

91. Visconti, P., Moore, G., Bailey, J., Leclerc, P., Connors, S., Pan, D., et al. (1995). Capacitation of mouse spermatozoa. II. Protein tyrosine phosphorylation and capacitation are regulated by a cAMP-dependent pathway. *Development* , 121: 1139-1150.

92. Vijayaraghavan, S., Goueli, S., Davey, M., & Carr, D. (1997). Protein Kinase A-anchoring Inhibitor Peptides Arrest Mammalian Sperm Motility. *J Biol Chem* , 272: 4747-4752.

93. Esposito, G., Jaiswal, B., Xie, F., Krajnc-Franken, M., Robben, T., Strik, A., et al. (2004). Mice deficient for soluble adenylyl cyclase are infertile because of a severe sperm-motility defect. *PNAS* , 10 (9): 2993-2998.

94. Lin, M., Lee, Y. H., Xu, W., Baker, M. A., & Aitken, R. J. (2006). Ontogeny of Tyrosine Phosphorylation-Signaling Pathways During Spermatogenesis and Epididymal Maturation in the Mouse. *Biol Reprod* , 75(4): 588-597.

95. Rodriguez-Miranda, E., Buffone, M. G., Edwards, S. E., Ord, T. S., Lin, K., Sammel, M. D., et al. (2008). Extracellular Adenosine 5'-Triphosphate Alters Motility and Improves the Fertilizing Capability of Mouse Sperm. *Biol Reprod* , 79(1): 164-171.

96. Hirano, Y., Shibahara, H., Obara, H., Suzuki, T., Takamizawa, S., Yamaguchi, C., et al. (2001). Relationships between sperm motility characteristics assessed by the computer-aided sperm analysis (CASA) and fertilization rates in vitro. *J Assist Reprod Genet* , 18(4): 213-218.

97. Tarnasky, H., Cheng, M., Ou, Y., Thundathil, J. C., Oko, R., & van der Hoorn, F. A. (2010). Gene trap mutation of murine outer dense fibre protein-2 gene can result in sperm tail abnormalities in mice with high percentage chimaerism. *BMC Dev Biol* , 10:67.